A ROLE FOR THE SHANK1 SCAFFOLD PROTEIN IN EXPERIENCE-INDUCED SYNAPTIC PLASTICITY AND MEMORY CONSOLIDATION

BY

SEAN M. COLLINS

DISSERTATION

Submitted in partial fulfillment of the requirements
for the degree of Doctor of Philosophy in Psychology
in the Graduate College of the
University of Illinois at Urbana-Champaign, 2018

Urbana, Illinois

Doctoral Committee:

Assistant Professor Roberto Galvez, Chair
Professor Janice Juraska
Associate Professor Joshua Gulley
Associate Professor Robert Wickesberg
Associate Professor Daniel Llano

ABSTRACT

The processes by which the brain acquires, stores, and retrieves external information has been an extensively researched field in psychology. Findings from these studies have overwhelmingly suggested that plasticity of neuroanatomical networks across development and during various experiences provide a critical mechanism mediating learning. Specifically, numerous studies have suggested dendritic spine plasticity across development and during learning as a likely process for memory consolidation. During early postnatal development, dendritic spine density increases in numerous sensory cortices, reaching a peak in adolescence, followed by a subsequent reduction in dendritic spine density to adult levels. In the hippocampus, dendritic spine density steadily increases during postnatal development, and plateaus in adulthood. Similar to the plasticity observed across development, increases in dendritic spine density occur in the neocortex and hippocampus following various learning paradigms, suggesting synaptic remodeling. While the anatomical properties for these forms of plasticity are well investigated, the underlying molecular processes remain largely unknown. Interestingly, recent studies have strongly suggested a role for SHANK1 in normal synaptic development and plasticity. SHANK1 is a scaffolding protein that is concentrated to the postsynaptic density (PSD) of excitatory synapses and is involved in the binding of glutamate receptors to their active zones. Previous developmental studies have demonstrated that SHANK1 is initially localized in the cytoplasm of neurons followed by an increased dendritic spine expression during periods of postnatal dendritic spine proliferation. Likewise, SHANK1 expression is increased across postnatal development in purified postsynaptic fractions, further suggesting a role in developmental properties of dendritic spines. Interestingly, global SHANK1 knockout (SHANK1 -/-) mice have also been shown to exhibit a reduction in dendritic spine density and increased immature dendritic spine phenotype.

Consistent with that observed in development, SHANK1 has been hypothesized to play an important role in learning-induced dendritic spine plasticity and cognition. SHANK1-/- mice exhibit marked impairments in contextual fear-conditioning and radial-arm-maze retention. Similarly, mice that overexpress SHANK1 exhibit impairments in both cued and contextual fear conditioning, further suggesting that appropriate SHANK1 regulation is crucial for normal cognition. Collectively, these studies strongly suggest a role for SHANK1 in developmental and learning-induced dendritic spine plasticity; however, a detailed examination of this has never been conducted. Furthermore, many of these studies genetically dysregulated SHANK1 from birth, thus a role for SHANK1 in normal adult learning-induced plasticity has not yet been examined. The studies in the present thesis further explored SHANK1 as an underlying mediator of dendritic spine plasticity in three specific aims. In Aim 1, a detailed examination of layer and cell-specific dendritic spine plasticity in S1 during distinct learning phases for WTEB was conducted. Findings from this study revealed no significant changes in dendritic spine density on layer III or layer V pyramidal cells at the specific time points examined across WTEB. In exploring these findings, we further discussed the implications of these findings, possible explanations as well as potential future studies to explore this research question. Aim 2 explored a role for SHANK1 expression during neuronal development, a well characterized period of dendritic spine plasticity. These studies demonstrated SHANK1 localization to neurons as well as astrocytes and microglia. Furthermore, this study also characterized cell-specific changes in SHANK1 expression during periods of developmental synaptic plasticity. Aim 3 expanded upon these findings to explore a role SHANK1 expression, during learning-induced neocortical dendritic spine plasticity and learning of WTEB. These studies demonstrated a transient increase in SHANK1 levels during periods of neocortical synaptic plasticity across WTEB. Collectively,

these studies further support a role of SHANK1 in the organization and remodeling of synaptic networks during development and learning. In so doing these studies also provided additional insight into potential specific mechanisms underlying developmental and experience-induced synaptic remodeling, deepening our understanding of memory consolidation within specific learning networks.

CONTENTS

INTRODUCTION

Dynamic Properties of Dendritic Spines

Dendritic spines are widely accepted as an underlying anatomical neuronal structure mediating learning and normal cognition. Changes in dendritic spine properties have been observed during development (development-induced) and across various learning paradigms (experience-induced) in brain regions such as the hippocampus and neocortex, that have been shown to mediate many forms of learning and memory (Fiala et al. 1998; Schachtele et al. 2011; Harris, Jensen, and Tsao 1992; Juraska 1982; Li et al. 2010; Turner and Greenough 1985; Chau, Akhtar, et al. 2014; Knott et al. 2002; Leuner, Falduto, and Shors 2003; Kleim et al. 1996; Greenough, Juraska, and Volkmar 1979). However, the underlying mechanisms by which dendritic spine plasticity occurs remain largely unknown. Further understanding of these mechanisms will not only broaden our knowledge of basic processes of learning, but also elucidate potential therapeutic targets for cognitive disorders. The current thesis outlines a series of experiments that explored the anatomical mechanisms mediating neocortical learning and a potential mechanism underlying both learning-and experience-induced anatomical plasticity, SHANK1 modulation.

Development-induced Dendritic Spine Plasticity

Dendritic spines are the primary site for receiving excitatory input on neurons (Kharazia et al. 1996). Furthermore, changes in dendritic spine structure and number have been theorized to be an underlying anatomical feature mediating learning and memory consolidation (Bailey, Kandel, and Harris 2015; Turner and Greenough 1985; Kleim et al. 1996; Chau, Akhtar, et al. 2014). For these reasons, many studies have focused on examining the structural formation and development of dendritic spines. While not completely understood, formation of individual

dendritic spines appears to follow a morphological change which greatly facilitates its influence on dendritic excitability. During initial formation of dendritic spines, long immature filopodia emerge from dendrites to make synaptic contacts (Fiala et al. 1998). 2-photon microscopy studies have demonstrated that these filopodia form and retract rapidly, and form connections with newly developed presynaptic varicosities, incorporating them into synaptic networks (Alvarez and Sabatini 2007). Through appropriate synaptic transmission, some filopodia transition into a mature morphology (Holtmaat et al. 2005). Mature dendritic spines are typically characterized as having a stubby or mushroom-like morphology, resulting in an increased dendritic spine head size (Bourne and Harris 2011; Spacek and Harris 1997). This swelling of spine heads is associated with an enlargement of the post-synaptic density (PSD) (Holtmaat et al. 2006). Specifically, studies have shown that the length of the PSD increases during development and in response to learning (Markus, Petit, and LeBoutillier 1987; Sirevaag and Greenough 1985; Fortin et al. 2010). PSD size is also positively correlated with glutamate receptor number, thus predictive of glutamatergic response of an individual synapse (Fortin et al. 2010; Brooks et al. 1991). Collectively, these studies suggest that a better understanding of development and learning can be obtained through examination of dendritic spine properties.

Developmental, structural, and functional plasticity of dendritic spines within sensory cortices and the hippocampus have been extensively studied largely due to their well-defined synaptic pathways and importance in learning and memory (Lomo 1971; Sloviter and Lomo 2012; Petersen 2003; Galvez, Weible, and Disterhoft 2007; Schenk and Morris 1985; Tseng et al. 2004; White 1974; Melo et al. 1997). Dendritic spines within many neocortical regions demonstrate an overproduction during development followed by a refinement of dendritic spine number in adolescence to early adulthood (Holtmaat et al. 2005; Juraska 1982; Li et al. 2010).

However, this dendritic spine overproduction/refinement has not been observed in the hippocampus. Rather, hippocampal dendritic spine density has been shown to gradually increase from birth, plateauing around postnatal day 60 (P60) in rodents (Harris, Jensen, and Tsao 1992; Fiala et al. 1998; Elibol-Can et al. 2014; Kirov, Goddard, and Harris 2004). During this process, anatomical analyses have demonstrated a developmental shift in dendritic spine morphology. Specifically, during the first two weeks of postnatal neocortical and hippocampal development, dendritic spines exhibit a dynamitic transition from a primarily filopodia morphology to mature dendritic spines (Fiala et al. 1998; Orner et al. 2014; Dailey and Smith 1996; Collin, Miyaguchi, and Segal 1997; Schachtele et al. 2011). However, the specific molecular mechanisms mediating this developmental plasticity of dendritic spine density and morphology remains largely unknown.

Experience-induced Dendritic Spine Plasticity

One of the most prominent theories for neuroanatomical mechanisms mediating learning and memory is the remodeling of synaptic connections. In support of this theory, a myriad of learning paradigms has been shown to elicit increases in synaptic density in the neocortex and hippocampus. For example, enriched rearing induces robust increases in the number of synapses per neuron in primary visual cortex (Turner and Greenough 1985; Sirevaag and Greenough 1985). Likewise, individual whisker stimulation, increases synaptic density in the posterior medial barrel subfield of primary somatosensory cortex (Knott et al. 2002). Furthermore, motor learning paradigms such as acrobat conditioning, where animals are trained to traverse a series of complex obstacles, increase the number of synapses per neuron in motor regions such as primary motor cortex and cerebellum (Kleim et al. 1996; Federmeier, Kleim, and Greenough 2002). Consistent with these studies, associative learning paradigms also induce increases in dendritic

spine number. For example, eyeblink conditioning (EBC), an associative learning paradigm that will be discussed in more detail below, has been shown to increase synaptic density in the stratum radiatum of CA1 and dentate gyrus sub-regions of the hippocampus (Geinisman et al. 2001; Leuner, Falduto, and Shors 2003). Similarly, dendritic spine density in the nucleus accumbens is increased following contextual conditioning with amphetamine administration (Singer et al. 2016). Consistent with these findings, dendritic spine proliferation has been observed in the lateral amygdala, hippocampus, and anterior cingulate cortex following fear learning (Restivo et al. 2009; Dalzell et al. 2011; Heinrichs et al. 2013).

Interestingly, although these and other studies have demonstrated an increase in dendritic spine density with various experiences, it is generally accepted that this learning-induced increase in dendritic spine density is transient and with memory consolidation results in a remodeling of synaptic networks (Barnes and Finnerty 2010; Bailey, Kandel, and Harris 2015; De Roo et al. 2008). However, there have been very few anatomical studies that have observed and directly studied this learning-induced synaptic remodeling. Whisker trimming studies examining the effects of altering sensory stimuli have observed this process through the elimination of mature dendritic spines and increased number of new dendritic spines in primary somatosensory cortex (Holtmaat et al. 2006). However, this is a sensory deprivation paradigm, making analogies between this paradigm and learning difficult to decipher. Studies examining acquisition for an avoidance conditioning and water maze task have both demonstrated a transient increase in hippocampal dendritic spine density (O'Malley, O'Connell, and Regan 1998; O'Malley et al. 2000; Scully et al. 2012). However, this synaptic remodeling occurs several hours after acquisition of the task; making it unclear the exact role this would play in task acquisition, especially since most agree that the hippocampus is not a site of memory storage (Kim, Clark,

and Thompson 1995; Martel, Jaffard, and Guillou 2010; Takehara et al. 2002). Rather, it is generally accepted that the neocortex is one of the most likely sites for long-term memory storage.

One of the few studies that has attempted to directly examine this learning-induced neocortical synaptic remodeling in the neocortex was previously conducted by our laboratory using the whisker-trace-eyeblink (WTEB) conditioning paradigm (Chau, Prakapenka, et al. 2014). WTEB is a forebrain dependent learning paradigm where a neutral conditioned stimulus (CS - whisker stimulation) is paired, following a short stimulus free trace interval, with an unconditioned stimulus (US - mild periorbital eye shock) that elicits an unconditioned behavioral response (UR - eyeblink). This form of conditioning is dependent upon proper neuronal communication within both the hippocampus and neocortex (Galvez, Weible, and Disterhoft 2007; Tseng et al. 2004). Studies from our laboratory have demonstrated that acquisition for this task induces an increase in spiny stellate dendritic spine density in layer IV of primary somatosensory cortex (S1) that returns to pre-training levels with subsequent training (Chau, Prakapenka, et al. 2014). To our knowledge this study was the first anatomical study to provide supporting evidence for learning-induced synaptic remodeling (addition of new synaptic connections followed by the removal of extraneous synaptic connections, returning dendritic spine density to pre-training levels). However, this analysis was only conducted in layer IV of the neocortex. Studies from other laboratories have shown that experience induces plasticity across all six neocortical layers (Withers and Greenough 1989; Greenough, Volkmar, and Juraska 1973). Taken together, these studies provide strong evidence for neocortical synaptic remodeling as a process for memory consolidation but are lacking in characterizing the time

course for this remodeling in non-layer IV neocortical neurons or identifying a potential mechanism driving this plasticity.

The SHANK Family of Scaffold Proteins

Recent studies have suggested that one mechanism facilitating developmental and experience-induced synaptic plasticity resides in the modulation of the synaptic scaffold protein SHANK. SHANK has been reported to be predominantly localized within the post-synaptic density (PSD) of excitatory synapses (Sheng and Kim 2000) playing a critical role in anchoring of glutamate receptors. SHANK is comprised of several protein binding sites allowing for multiple areas of protein-protein interactions. These domains include an SRC Homology 3 (SH3) domain, PSD-95/Dlg/ZO-1 (PDZ) domain, sterile alpha motif (SAM) domain, proline-rich region, as well as multiple ankyrin repeats (Lim et al. 1999; Sheng and Kim 2000). SHANK has been demonstrated to interact with three of the four main types of glutamate receptors (AMPARs, NMDARs, and mGluRs). The SH3 region binds directly to GRIP that binds AMPARs, forming an AMPAR/GRIP/SHANK complex. Similarly, the SHANK PDZ domain forms a complex with both PSD-95 that binds to NMDARs, and the proline-rich region of Homer that binds mGluR (Tu et al. 1999; Naisbitt et al. 1999; Lim et al. 1999).

SHANK is comprised of three separate proteins: SHANK1, SHANK2, and SHANK3, each slightly varying in structure and localization. SHANK3 mRNA is primarily concentrated in the heart with moderate levels in the brain and spleen (Lim et al. 1999). During postnatal development, SHANK3 mRNA expression in the brain is low at birth, following an increase during early development (Bockers et al. 2004). In cultured neurons SHANK3 protein increases from 1 to 14 days in vitro (DIV) but the developmental profile of SHANK3 in vivo is less clear (Halbedl et al. 2016). In recent years, SHANK3 dysregulation has been heavily implicated in

Autism Spectrum Disorder (ASD). Mutations to SHANK3 have been observed in a subset of ASD patients and SHANK3 mutant mice demonstrate many abnormalities observed in ASD patients such as repetitive behaviors, abnormalities in social behaviors, cognitive impairments, and immature dendritic spine morphology (Betancur and Buxbaum 2013; Durand et al. 2012; Wang et al. 2011; Peca et al. 2011; Mashayekhi et al. 2016). Like SHANK3, SHANK2 mRNA is also expressed in the periphery and brain. At birth, neuronal SHANK2 protein is expressed at high levels within the cytoplasm of cell bodies and steadily accumulates in the PSD during postnatal development. Additionally, the presence of SHANK2 in the PSD precedes NMDA receptor insertion, implying an important role for SHANK in the developmental organization of glutamatergic signaling (Boeckers et al. 1999).

Interestingly unlike SHANK3 and SHANK2, SHANK1 mRNA is exclusively found in brain, suggesting its potential role in brain specific processes (Boeckers et al. 1999; Lim et al. 1999). Overall, SHANK1 protein levels have been shown to be consistent across postnatal development. However, like SHANK2, SHANK1 is initially localized in the cytoplasm of cell bodies at birth and is transported to the postsynaptic density during postnatal neuronal development (Lim et al. 1999; Boeckers et al. 1999). Due to its brain specific expression pattern, the remainder of this introduction and thesis will focus exclusively on SHANK1.

SHANK1 Modification of Dendritic Spines

SHANK1 expression has been widely implicated in regulating the structure of dendritic spines. Studies have demonstrated that SHANK1 overexpression increases dendritic spine length and width in vitro (Sala et al. 2001; Hung et al. 2008). Consistent with these findings, RNAi knockdown of SHANK1 decreases dendritic spine density in cultured hippocampal neurons (Grabrucker et al. 2011). Similarly, SHANK1 knockout mice also exhibit decreased CA1

hippocampal dendritic spine density (Hung et al. 2008). Collectively, these studies provide evidence for a brain-specific role of SHANK1 in mediating dendritic spine density and structure.

Implications for SHANK1 in Learning

The role SHANK1 plays in synaptic plasticity appears to be implicated in performance of numerous learning tasks. For example, SHANK1 knockout mice demonstrate marked impairments in long-term retention of an eight-arm radial maze. Furthermore, these SHANK1 knockout mice are impaired in their ability to recall contextual fear conditioning (Hung et al. 2008). Conversely, mice that overexpress SHANK1 have been shown to demonstrate impaired cued and contextual fear conditioning. In addition, SHANK1 overexpression also impairs late phase long-term potentiation (LTP), a molecular mechanism believed to facilitate learning which is dependent on gene transcription and synthesis of new proteins (Pick, Malumbres, and Klann 2012). These studies imply an importance for appropriate regulation of SHANK1 in associative learning and mechanisms for learning.

SHANK1 Dysregulation in FXS

In addition to its role in dendritic spine plasticity and learning, SHANK1 dysregulation has been found to be associated with the Fragile X Mental Retardation Syndrome (FXS). FXS is the leading form of inherited mental retardation and the most prominent form of Autism (Tassone et al. 2012). It is caused by the transcriptional silencing of the Fragile X Mental Retardation Protein (FMRP). Interestingly, FMRP acts as a negative regulator of SHANK1 translation via interaction with SHANK1 mRNA's 3' untranslated region (UTR) (Zhang et al. 2014). Thus, in the absence of FMRP, as observed in FXS, SHANK1 brain protein expression is upregulated compared to controls (Schutt et al. 2009). FXS anatomical studies have further found the syndrome to be

associated with an increased density of immature dendritic spines, consistent with SHANK1 overexpression studies on dendritic spine properties (see SHANK1 Modification of Dendritic Spines above) (Grossman et al. 2010; Galvez, Gopal, and Greenough 2003; Galvez and Greenough 2005; Irwin et al. 2001). These findings collectively suggest a possible role for SHANK1 dysregulation mediating FXS behavioral and cognitive abnormalities, while further support a role for SHANK1 in synaptic plasticity, neuronal development and cognition.

Conclusion

The above studies provide evidence for the regulation of SHANK1 as a mechanism for developmental and experience-induced neuronal plasticity critical for normal cognition and learning. Additionally, the brain-specific localization of SHANK1 makes this scaffold protein a particularly attractive candidate for further exploration of developmental and learning-induced dendritic spine remodeling. The studies discussed below further explore learning-induced dendritic spine plasticity and SHANK1 as a mediator of this plasticity in the following carefully designed aims. In Aim 1, a detailed examination of layer and cell-specific dendritic spine plasticity in S1 during distinct learning phases for WTEB was conducted. This aim expands upon the studies of Chau et al., (2014), while providing a more complete assessment of learning induced anatomical neocortical plasticity. Aim 2 characterized SHANK1 developmental brain expression in different cell types, providing a potential role in brain neuronal and glial developmental plasticity. Aim 3 expands upon these findings to determine if SHANK1 facilitates acquisition for WTEB. In this study, SHANK1 was first determined to exhibit differential expression in S1 during periods of WTEB induced synaptic plasticity. Following this initial assessment, the role of SHANK1 in WTEB acquisition was further assessed through S1 local shRNA knock down. Collectively, these studies have further elucidated a role for SHANK1 in

the organization and re-organization of synaptic networks during development and learning respectively. In so doing, these studies further provide insight into specific mechanisms underlying developmental and experience-induced synaptic remodeling deepening our understanding of memory consolidation within specific learning networks.

CHAPTER I: Analysis of Dendritic Spine Plasticity on Layer III and Layer V Pyramidal Cells in Primary Somatosensory Cortex during Neocortical-dependent Associative Learning

Abstract

The neocortex is generally accepted to be a site for long-term memory storage. In support of this, classic studies have demonstrated robust increases in dendritic spines following various learning experiences. These studies, along with multiple learning theories have further suggested that remodeling of synaptic connections, characterized by transient increases in dendritic spines, underlies memory consolidation. Surprisingly, few studies have directly examined dendritic spine remodeling (i.e. transient increase in dendritic spines) across learning. In one of the few studies that has anatomically explored this hypothesis, our laboratory has demonstrated that dendritic spines exhibit a transient increase during learning of whisker-trace-eyeblink conditioning (WTEB) in primary somatosensory cortex (S1). WTEB is an associative learning paradigm in which a neutral conditioned stimulus (CS - whisker stimulation) is paired with an unconditioned stimulus (US - mild periorbital eye-shock), following a brief stimulus-free trace interval. While anatomical studies with this paradigm have provided some of the first evidence for learning-induced synaptic remodeling, plasticity was only examined for one cell type in layer IV of S1. Thus, a detailed analysis of synaptic remodeling across the different neocortical layers has not yet been explored. To address this, the current study used Golgi-Cox impregnation to examine dendritic spine density on layer III and layer V pyramidal cells within S1 across behaviorally distant time-points of WTEB. These analyses revealed no significant leaning-induced changes in dendritic spine plasticity in either of these cell types. However, potential limitations in the experimental design could have masked or even prevented detection of any

learning-induced dendritic spine plasticity. In the current study it was not possible to determine which cells were receiving input from the specific barrels, thus potentially increasing detection variability. Furthermore, due to the necessary post-mortem analysis for golgi detection, the specific time window for dendritic spine plasticity on these specific cell types may have been missed. To better determine the time course for learning-induced dendritic spine plasticity, we suggest for subsequent studies to utilize real time imaging techniques such as two-photon (2P) microscopy. Then once specific time points of dendritic spine plasticity are determined, subsequent more detailed, cell specific morphological analyses can be conducted using golgi impregnation. These future studies would help ensure the success of these studies while providing a more complete representation of synaptic remodeling during learning and memory consolidation.

Introduction

One of the most prominent theories for neuroanatomical mechanisms underlying neocortical memory consolidation is the addition of new synaptic connections. In support of this theory, various learning paradigms have been shown to elicit increases in synaptic density across the neocortex. For example, enriched rearing induces robust increases in the number of synapses per neuron in primary visual cortex and sensory stimulation, through whisker stimulation, increases synaptic density in the posterior medial barrel subfield of primary somatosensory cortex (Turner and Greenough 1985; Knott et al. 2002). Likewise motor learning paradigms such as acrobat conditioning, where animals are trained to traverse a series of complex obstacles, increase the number of synapses per neuron in motor regions such as primary motor cortex and cerebellum (Kleim et al. 1996; Federmeier, Kleim, and Greenough 2002). Consistent with these studies, the associative learning paradigm eyeblink conditioning (EBC) has been shown to increase synaptic density in the neocortex and hippocampus (Geinisman et al. 2001; Bakin, South, and Weinberger 1996; Heinrichs et al. 2013; Leuner, Falduto, and Shors 2003; Chau, Prakapenka, et al. 2014).

Interestingly, although these and other studies have demonstrated an increase in dendritic spine density with learning, it is generally accepted that this learning-induced increase in dendritic spine density is transient and with memory consolidation results in a remodeling of synaptic networks (Barnes and Finnerty 2010; De Roo et al. 2008; Bailey, Kandel, and Harris 2015). However, there have been very few anatomical studies that have observed and directly studied this learning-induced synaptic remodeling. Whisker trimming studies examining the effects of sensory deprivation have observed this process through the elimination of mature dendritic spines and increased number of new dendritic spines in primary somatosensory cortex (Holtmaat et al. 2006). However, this is a sensory deprivation paradigm, making analogies

between this paradigm and learning difficult to determine. Studies examining acquisition for an avoidance conditioning and water maze task have both demonstrated a transient increase in hippocampal dendritic spine density (O'Malley, O'Connell, and Regan 1998; O'Malley et al. 2000; Scully et al. 2012). However, this synaptic remodeling occurs several hours after acquisition of the task; thus, making it unclear the exact role this would play in task acquisition. Furthermore, as most agree the hippocampus is not a site of memory storage (Kim, Clark, and Thompson 1995; Martel, Jaffard, and Guillou 2010; Takehara et al. 2002). Rather, it is generally accepted that the neocortex is the most likely site for memory storage.

Recent studies from our laboratory have demonstrated remodeling of neocortical dendritic spines during acquisition and consolidation of whisker-trace-eyeblink (WTEB) conditioning (Chau, Prakapenka, et al. 2014). WTEB is a forebrain dependent associative learning paradigm where a neutral conditioned stimulus (CS - whisker stimulation) is paired, following a short stimulus free trace interval, with an unconditioned stimulus (US - mild periorbital eye shock) that elicits a behavioral response (eyeblink). This form of conditioning is dependent upon proper neuronal communication within both the hippocampus and neocortex (Galvez, Weible, and Disterhoft 2007; Tseng et al. 2004). Studies from our laboratory have demonstrated that acquisition for this task induces an increase in spiny stellate dendritic spine density in layer IV of primary somatosensory cortex (S1) that returns to pretraining levels with subsequent training (Chau, Prakapenka, et al. 2014). To our knowledge this study was the first anatomical demonstration of learning-induced synaptic remodeling (addition of new synaptic connections followed by the removal of extraneous synaptic connections, returning dendritic spine density to pretraining levels). However, this analysis was only conducted in layer IV of the neocortex. Studies from other laboratories have shown that experience induces plasticity across

all six neocortical layers (Withers and Greenough 1989; Greenough, Volkmar, and Juraska 1973). However, a time-dependent anatomical dendritic spine analysis from different cell types in different neocortical layers has never been conducted. Therefore, the present study examined dendritic spine plasticity in layer III and layer V pyramidal cells during different behavioral phases of WTEB.

Materials and Methods

Animals

Male C57BL/6 mice, aged 3-6 months, (n = 50) were bred in house and housed with littermates until day of surgery at which time they were transferred to individual standard clear laboratory cages (12" x 12" x 12"). Mice were maintained on a 12:12 light/dark cycle with food and water available *ad libitum*. All animal procedures were performed in compliance with the Institutional Animal Care and Use Committee (IACUC) at the University of Illinois Urbana-Champaign.

Surgery

The surgical procedure was performed as previously conducted (Galvez et al. 2009). Briefly, mice were anesthetized via intraperitoneal (i.p.) administration of a ketamine/xylazine cocktail (ketamine 1 mg/kg; xylazine 6 mg/kg). Once anesthetized fur was shaved from the head and mice were secured in a stereotaxic apparatus. The scalp was cleaned using a sterile alcohol prep pad followed by a betadine antiseptic scrub. Two percent Lidocaine was then injected under the skin at the incision site for local anesthesia. A small (~2 cm) incision was made across the midline of the head to expose the skull. A "headbolt" containing two Teflon-coated steel wires and an uncoated steel ground wire was secured to the skull. Coated wires were fed under the scalp to the periorbital region and the coating was removed from the contact site around the eye.

The ground wire was then tightly wrapped around a screw inserted into the surface of the skull. Upon surgery completion, mice received an injection of carprophin (5 mg/ml, 0.3 ml) and were given a minimum of 7 days to recover before behavioral training.

Behavioral training

Mice were trained as previously conducted (Galvez et al. 2009). Briefly, conditioning was performed in standard clear laboratory cages within a large sound attenuated chamber. Headbolts were connected to free-hanging tethers that provided whisker and periorbital stimulation as well as record eyelid closure using a custom LabView program. On the day preceding training mice were habituated to the chamber and tether for 10 minutes. Following the habituation day, mice were exposed to daily conditioning sessions consisting of 30 conditioning trials separated by 15-25 s intertrial intervals. Individual trials consisted of a 250 ms whisker stimulation (CS) paired with a 100 ms periorbital eyeshock (0.1 – 0.5 mA periobital square wave shock, 60 Hz, 0.5 ms pulses; US). The CS and US were temporally separated by a 250 ms stimulus-free trace interval. A live feed from a camera on the tether focused on the eye was converted into a binary image and analyzed with the LabView program in real time. Eyelid closure resulted in a change in area of the binary image. For individual mice, a threshold change in area was established for classification of CRs that corresponded to approximately 2 standard deviations from baseline. A CR was defined as a suprathreshold deviation of area of the binary image from baseline occurring after CS onset and before US onset. Mice were randomly assigned to trace-paired (n = 20) or pseudo-unpaired (n = 21) conditioned group. Trace-paired mice were further randomly divided into either an acquisition (ACQ, n = 8), learned, (LRD, n = 7), or over-trained (OT, n = 6) group. Mice in the ACQ group were trained until they exhibited three CRs in five consecutive trials. LRD mice were trained until they exhibited four CRs in five consecutive trials and OT

mice were trained until they performed two consecutive days of exhibiting four CRs in five consecutive trials. Pseudo-conditioned controls were randomly yoked to trace conditioned mice so that they received the same number of CS and US trials but in an unpaired order to account for stimulation-induced plasticity. Cage controls (CC, n = 7) did not undergo surgery or conditioning and were collected at the same time as conditioned mice.

Golgi processing

Mice were given a lethal dose of sodium pentobarbital 1 h after the final conditioning session. Mice were then transcardially perfused with 0.1 phosphate-buffered saline (PBS), brains were collected and processed as previously described (Galvez, Gopal, and Greenough 2003; Comery et al. 1997). Briefly, whole brains were placed into a standard Golgi-Cox solution for 14 days. After, full impregnation, brains were embedded in 10% celloidin and sectioned at 175 µm into 100% butanol. Tissue was further processed in ammonium hydrodide for 30 min followed by a 30 min incubation in Kodak rapid fixer and cover-slipped using Permount.

Layer-specific analyses of spine density in primary somatosensory cortex

Spine density for 8-10 layer III and layer V pyramidal cells were assessed for each mouse. Layer III cells were characterized as having cell bodies located in layer III with Y-shaped apical bifurcations in layer II and dendrites terminating in layer I (Fig. 2a). Layer V pyramidal cells were characterized as having cell bodies located in layer V with apical dendrites terminating in layer I (Fig. 2b). Furthermore, due to prior studies suggesting that layer III is more susceptible to learning-induced plasticity (Hardingham, Gould, and Fox 2011; Kuhlman et al. 2014a), a more extensive spine analysis on layer III basilar dendrites was conducted. Layer III basilar dendrites primarily receive input from within layer III. For these analyses, spine counts were performed for

each dendritic branch order (second order basilar, third order basilar, and fourth order basilar) at 100x magnification over dendritic segments ranging from 10-15 µm. Spine counts were further assessed for each spine morphology: Immature (filopodia-like), Intermediate (thin with bulbous head), or mature (stubby, mushroom-like, or multiple heads) and then divided by the dendritic length to obtain morphology specific density (#/µm).

Statistics

Behavioral analysis was conducted with a one-way ANOVA comparing day to criterion between each of the learning groups. Analyses for total spine density was conducted between learning groups using one-way ANOVA each cell type. Dendritic spines on basilar dendrites of layer III pyramidal cells were further analyzed using separate one-way ANOVAs comparing each morphology on second order, third order, and fourth order basilar dendrites.

Results

WTEB behavioral analysis

A one-way ANOVA comparing %CRs on day of criterion between trace- and pseudo-conditioned subjects demonstrated a significant effect between groups (Fig 3; $F_{(5,39)} = 39.56$, $p < .0001$). Subsequent Tukey post-hoc analyses demonstrated that the trace-conditioned LRD and OT groups exhibited significantly more %CRs on day of criterion compared to their respective yoked controls (LRD: ($t_{(39)} = 6.90$, $p < .0001$); OT: ($t_{(39)} = 8.79$, $p < .0001$)). Furthermore, the OT group exhibited significantly more %CRs than the ACQ ($t_{(39)} = 8.34$, $p < .0001$) and LRD groups ($t_{(38)} = 4.63$, $p = .0005$), and the LRD group exhibited significantly higher %CRs than the ACQ group ($t_{(39)} = 4.64$, $p = .0005$).

Analysis of dendritic spine density during WTEB

Analyses of total dendritic spine density of layer III and layer IV pyramidal cells revealed no significant changes in dendritic spine density across any learning time-point of WTEB (Fig 4a-b). Further analyses of layer III basilar dendrites revealed no significant changes in dendritic spine density for any morphology at any order of dendritic branch (Fig 4c-f).

Discussion

Many classic studies have demonstrated synaptic plasticity following various learning experiences across all layers within the neocortex (Turner and Greenough 1985; Knott et al. 2002; Kleim et al. 1996). Furthermore, studies from our laboratory have demonstrated a transient increase in dendritic spine density following WTEB on layer IV S1 spiny stellate cells suggesting remodeling of neocortical synaptic networks, a well-accepted theory of memory consolidation (Chau, Prakapenka, et al. 2014). However, this previous study was conducted exclusively in layer IV. Thus, synaptic reorganization in other neocortical layers across associative learning has not been examined. Therefore, the current study examined neocortical dendritic spine plasticity in layer III and layer V pyramidal cells across distinct time-points during WTEB.

Analyses from the current study observed no significant changes in total dendritic spine density in layer III or layer V pyramidal cells between any time-points during WTEB. Previous studies have demonstrated dramatic experience induced plasticity in layer III (Hardingham, Gould, and Fox 2011; Ma et al. 2016; Kuhlman et al. 2014b) and previous studies from our laboratory have demonstrated a transient increase in immature, and intermediate dendritic spines across WTEB but not mature spines (Chau, Prakapenka, et al. 2014). Therefore, further analyses comparing dendritic spine density of each morphology (immature, intermediate, and mature) at each of the three measured dendritic branch orders (second, third, and fourth) of layer III

pyramidal cells were conducted. These analyses also revealed no significant differences between any learning time-points. Collectively, findings from the current study suggest dendritic spine plasticity within layer III and layer V pyramidal cells within S1 exhibit a different dendritic spine density profile during WTEB compared to layer IV spiny stellate cells. However, several limitations of the present study may have contributed to this lack of observed plasticity.

Prior studies from our laboratory demonstrating dendritic spine remodeling during WTEB were conducted exclusively in layer IV spiny stellate cells that had dendrites located within whisker barrels in layer IV (Chau, Prakapenka, et al. 2014), the primary input of sensory thalamic projections (Bernardo and Woolsey 1987; Killackey and Ebner 1973; Killackey and Belford 1979). These cells have been demonstrated to primarily project to cells in the supragranular region of S1 (layer II/III) within the same whisker barrel column which then subsequently synapse largely with cells in the subgranular region (layer V/VI) (Lubke et al. 2000; Gottlieb and Keller 1997). Therefore, whisker input is largely integrated within these barrels. Given that the process of tissue preparation in the current study made it impossible to identify individual barrel columns, determining the specific barrel column localization for the examined neurons was not possible. Therefore, this lack of specificity may have masked learning-induced spine plasticity in cells receiving input directly from the barrel column in the present study.

Studies exploring experience induced synaptic remodeling in real time in live animals utilizing two-photon (2P) microcopy have further demonstrated that dendritic spine plasticity within S1 is a dynamic process with some dendritic spines forming and being eliminated in a matter of minutes while others persisting for months (Holtmaat et al. 2006; Wilbrecht et al. 2010). In addition, various experiences have been shown to elicit changes in this dynamic

process. For example, layer II/III S1 pyramidal cells demonstrate an increase in elimination but no changes in formation of dendritic spines during the first week following whisker trimming (Ma et al. 2016). Other studies have demonstrated a significant increase in formation of layer II/III S1 dendritic spines only during day 8 of a whisker-dependent discrimination task and an increase in spine loss during day 16 of training (Kuhlman et al. 2014a). Interestingly, in spite of experience-induced dynamitic dendritic spine formation and elimination, the overall spine density has been shown to remain unchanged on apical tufts of layer V S1 pyramidal cells (Holtmaat et al. 2006). This dynamic nature of formation and elimination of dendritic spines along with the timing for these processes within S1, may have contributed to the lack of observed plasticity in the present study. In the current study spine analyses were conducted utilizing a golgi stain, thus limiting analyses to the specific time point when the animal was sacrificed. Therefore, hindering detection of learning-induced changes in formation, elimination, and stability of individual dendritic spines.

Current research exploring learning-induced dendritic spine remodeling typically employs either golgi staining, electron microscopy (EM), or 2P microscopy. While golgi and EM have some advantages in visualization and detection abilities, these methods require sacrifice of the subjects thus making it impossible to analyze dendritic spine formation and elimination in real time. Analyses using 2P microscopy can assess this plasticity in real time; however, this methodology lacks the resolution needed to reliably characterize morphological features of dendritic spines. In the present study mice were sacrificed 1 hr after behavioral criterion was met for each subject; however, at least one prior study has demonstrated learning induced remolding of synaptic networks may occur up to 6 hours following learning (O'Malley et al. 2000). Therefore, synaptic remodeling of different cell types may occur at different times following a

learning experience. Future studies should explore the specific time course of synaptic remodeling of layer III and layer V pyramidal cells through a 2P microscopy analysis during WTEB at several time-points during learning. By assessing these changes across a larger time-frame, these studies would provide a time course of synaptic remodeling in multiple cell types allowing for subsequent golgi or EM studies to conduct a more extensive morphological analysis of dendritic spines during pre-defined time-points of observed synaptic plasticity. These studies would begin to develop a more complete representation of structural dendritic spine remodeling during WTEB. In so doing, these studies will further develop our understanding of the time-course of synaptic reorganization during learning and memory consolidation.

Figures

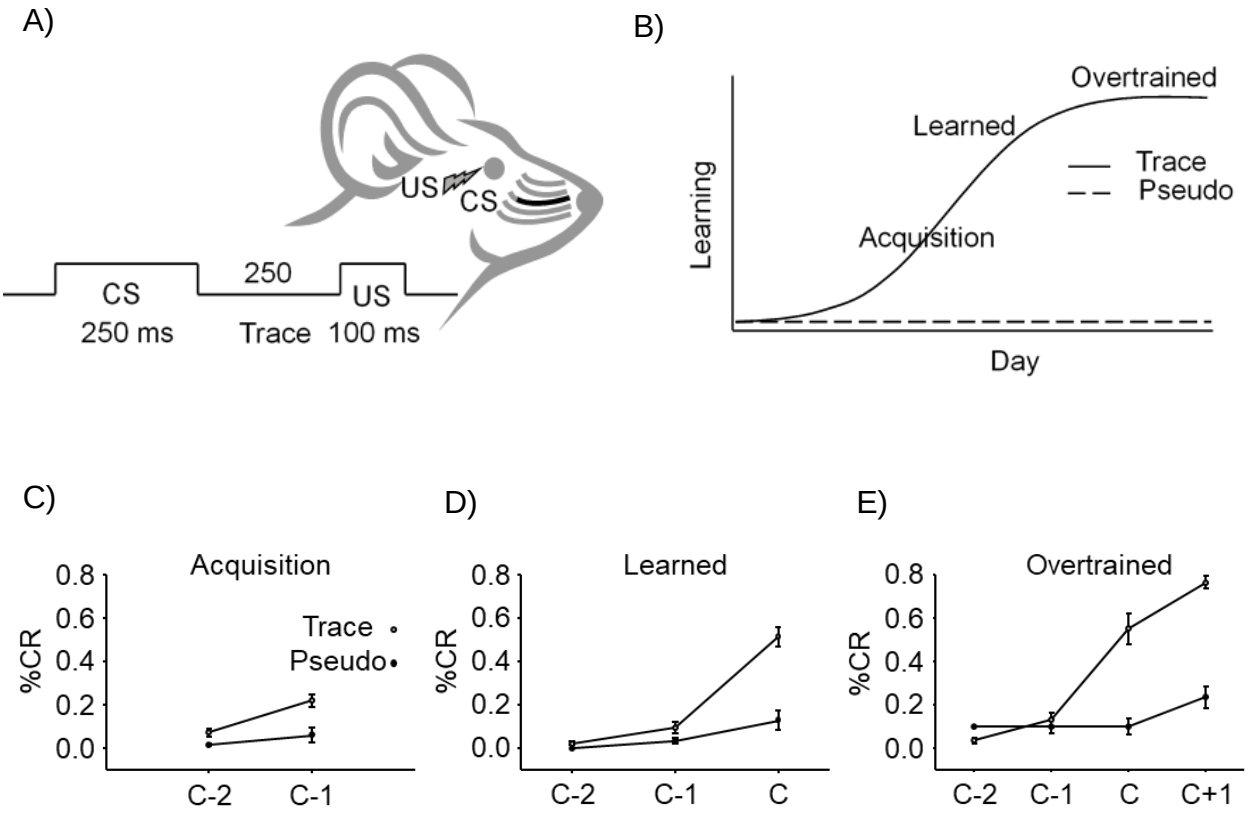

Figure 1. Behavioral analysis of neocortical-dependent whisker-trace-eyblink conditioning (WTEB). A) Schematic of temporal CS-US pairing during WTEB. Whisker stimulation (CS, 250 ms) is paired with a mild periorbital eye shock (US, 100 ms) following a stimulus free interval (trace, 250 ms). B) Theoretical WTEB learning curve demonstrating an increase in learning as a function of training comparing trace and pseudo conditioned subjects with the theoretical points for each learning time-point (Acquisition, Learned, Overtrained). C-E) WTEB performance comparing trace and pseudo conditioned subjects for each learning time-point. Note: Day C represents day of criterion for the Learned group.

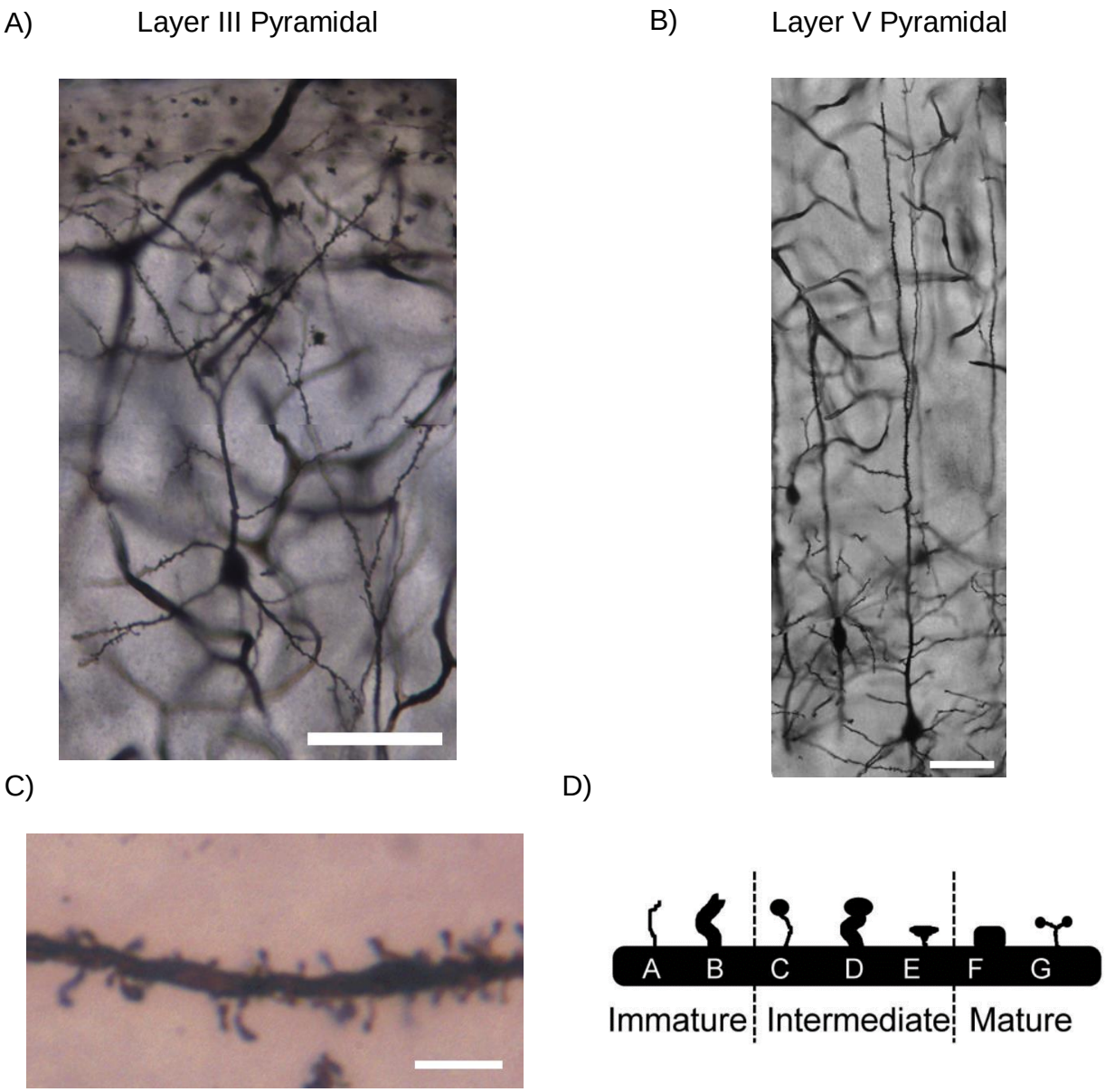

Figure 2. Representative images of Gogi-Cox stained S1 neocortical pyramidal neurons. A) Representative image of layer III S1 pyramidal cell at 20x magnification; scale bar = 20 µm. B) Representative image of layer V S1 pyramidal cell at 10x magnification; scale bar = 20 µm. C) Image depicting dendritic spine morphologies at 100x magnification; scale bar = 5 µm. D) Representative illustration of immature, intermediate and mature spine morphologies.

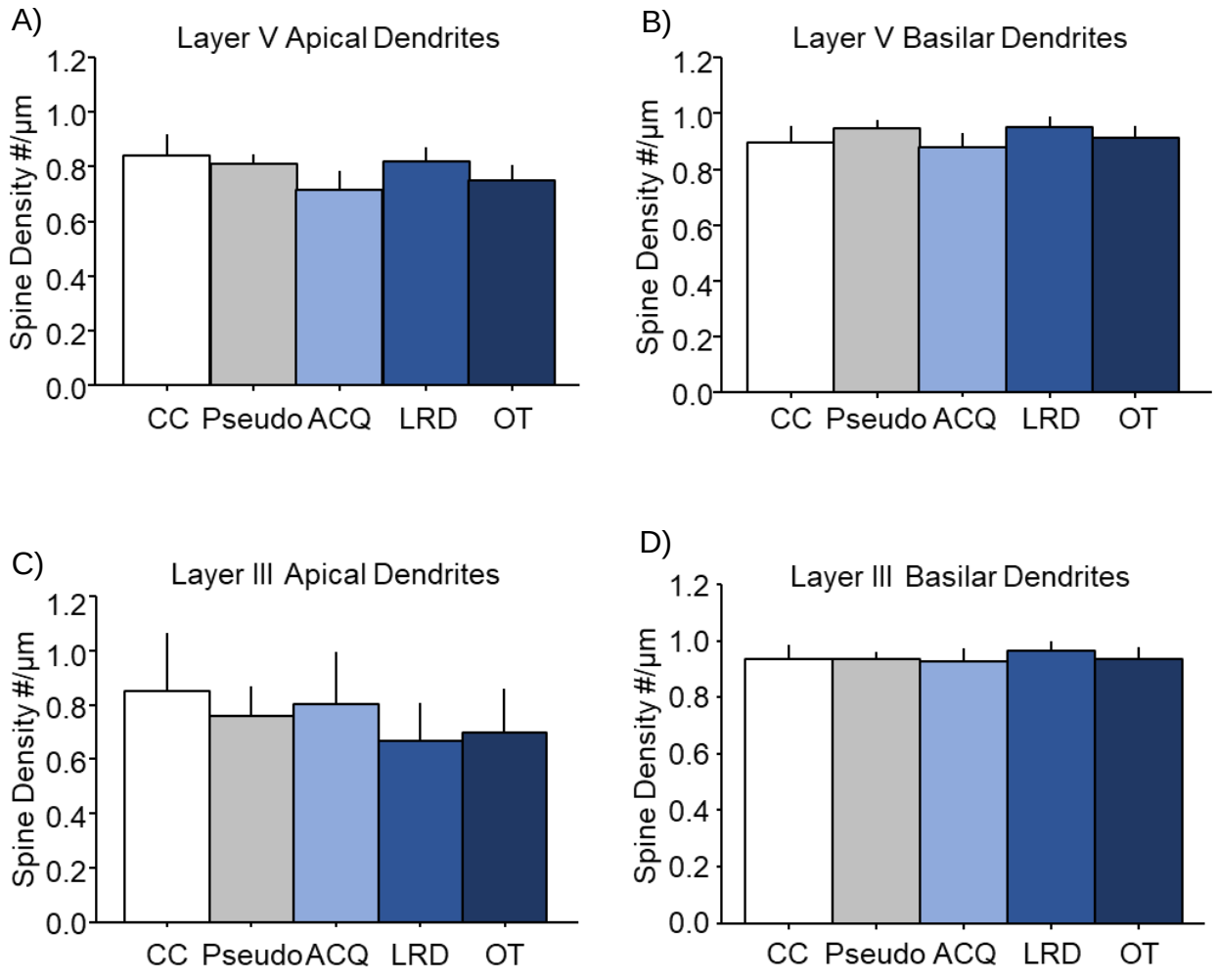

Figure 3. Apical and basilar dendritic spine density on S1 layer V and layer III pyramidal cells remains unchanged during learning of WTEB. A-D) Analyses of apical and basilar dendritic spine number/µm revealed no significant differences between cage controls (CC), pseudo-conditioned controls (Pseudo), or trace-conditioned acquisition (ACQ), learned (LRD), or overtrained (OT) subjects.

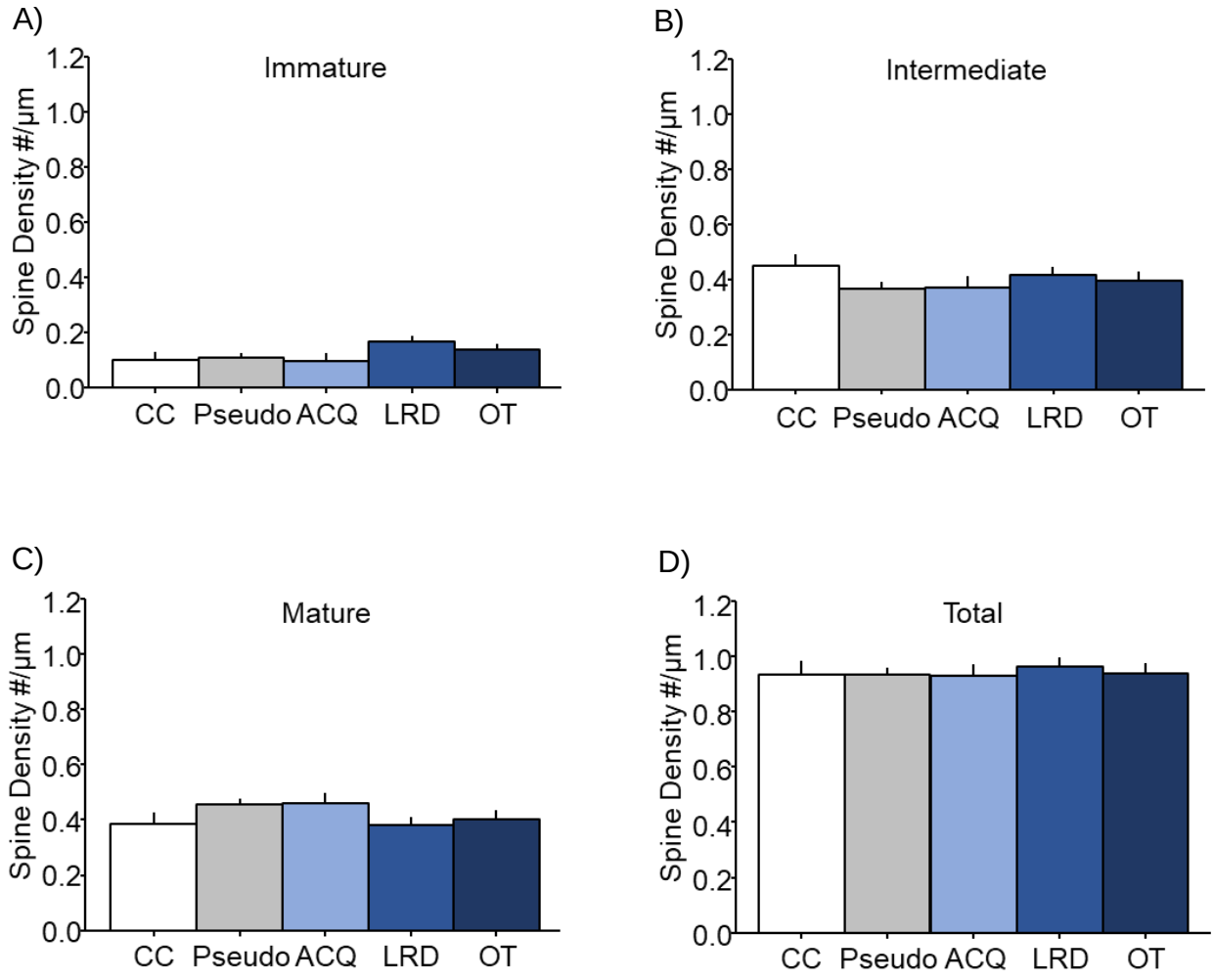

Figure 4. Combined basilar dendritic spine density S1 layer III pyramidal cells remains unchanged during learning of WTEB. A-D) Analyses of dendritic spine number/µm for each morphology (immature, intermediate, and mature) as well as all morphologies combined (total) revealed no significant differences between cage controls (CC), pseudo-conditioned controls (Pseudo), or trace-conditioned acquisition (ACQ), learned (LRD), or overtrained (OT) subjects.

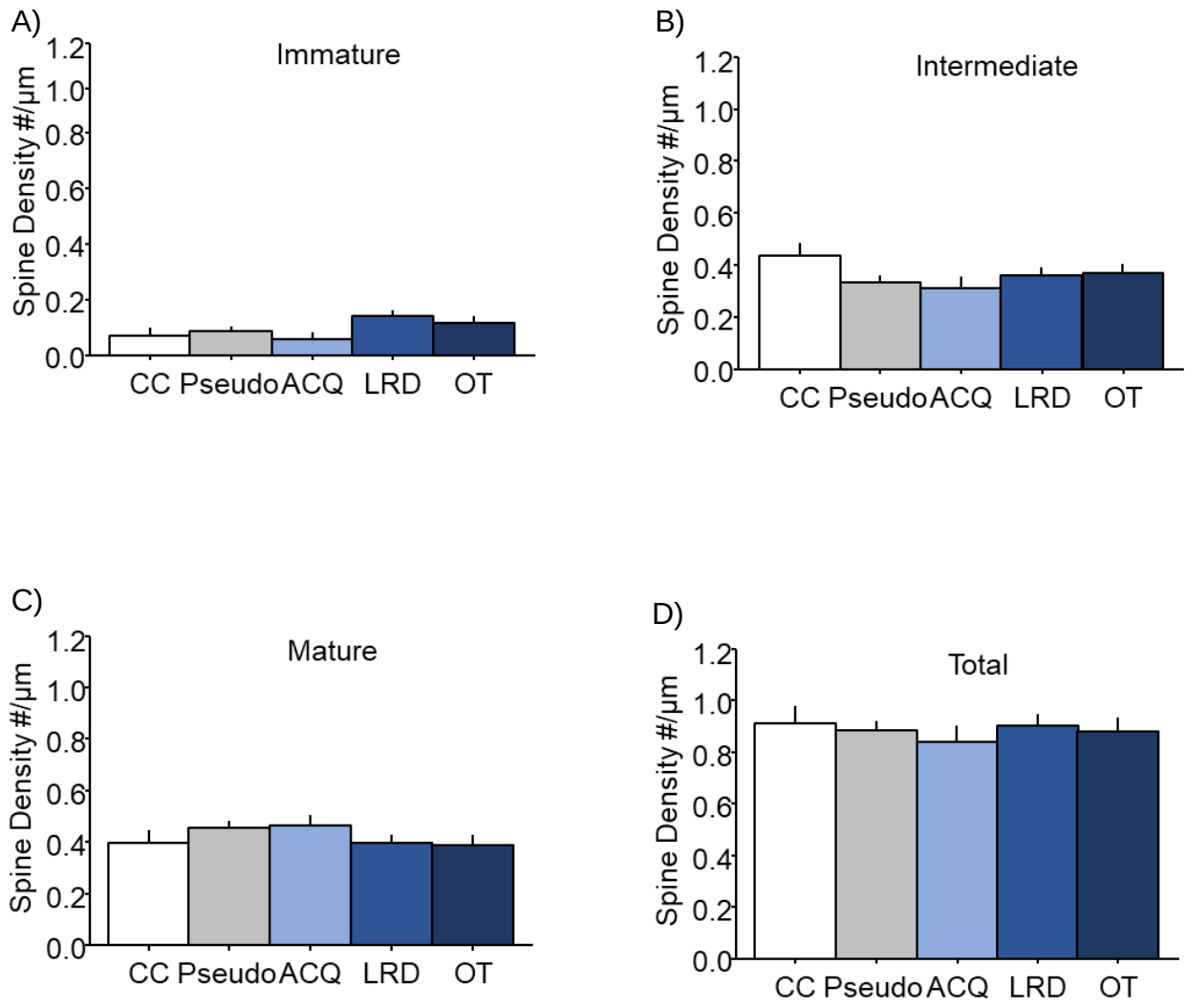

Figure 5. Second order basilar dendritic spine density S1 layer III pyramidal cells remains unchanged during learning of WTEB. A-D) Analyses of dendritic spine number/µm for each morphology (immature, intermediate, and mature) as well as all morphologies combined (total) revealed no significant differences between cage controls (CC), pseudo-conditioned controls (Pseudo), or trace-conditioned acquisition (ACQ), learned (LRD), or overtrained (OT) subjects.

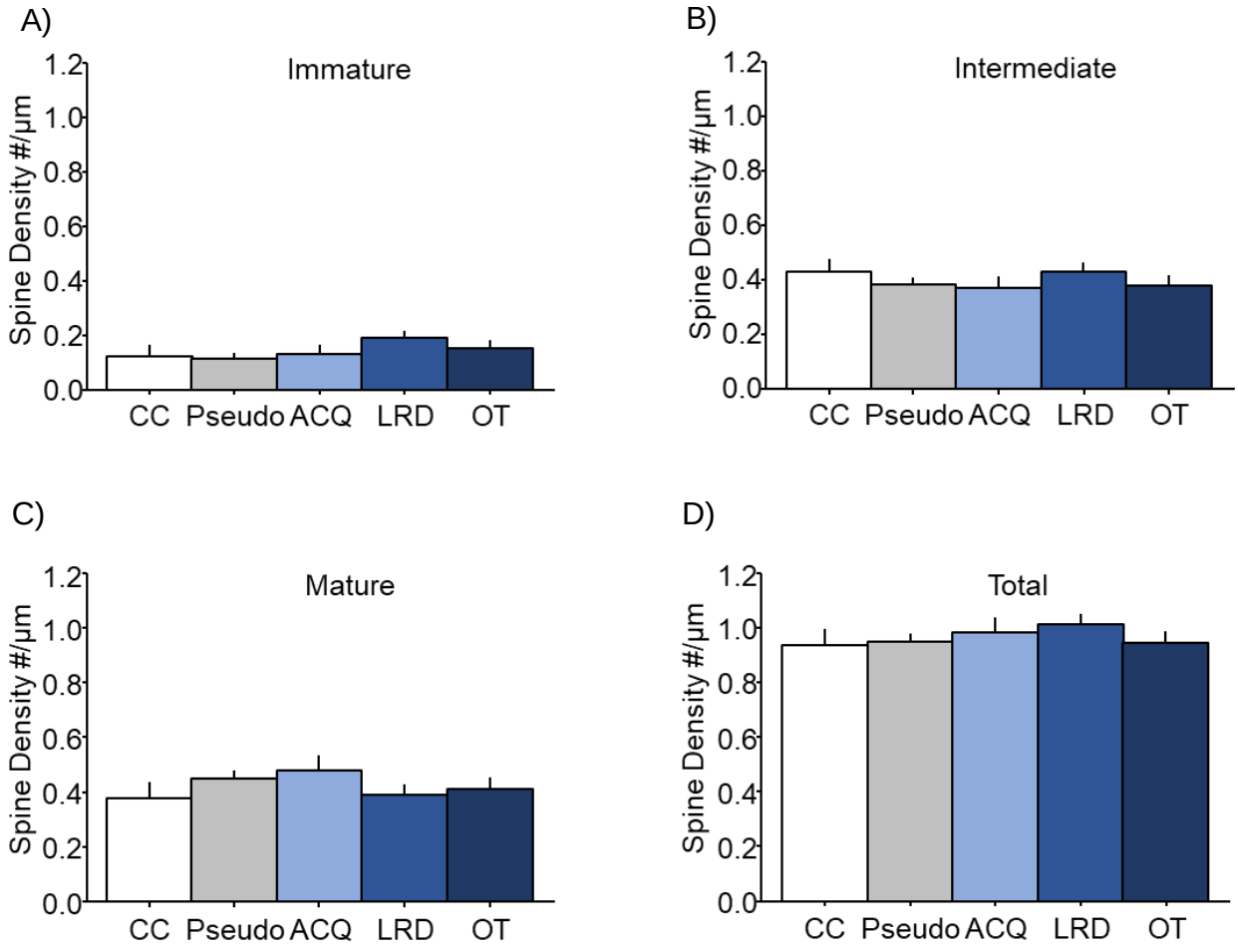

Figure 6. Third order basilar dendritic spine density S1 layer III pyramidal cells remains unchanged during learning of WTEB. A-D) Analyses of dendritic spine number/µm for each morphology (immature, intermediate, and mature) as well as all morphologies combined (total) revealed no significant differences between cage controls (CC), pseudo-conditioned controls (Pseudo), or trace-conditioned acquisition (ACQ), learned (LRD), or overtrained (OT) subjects.

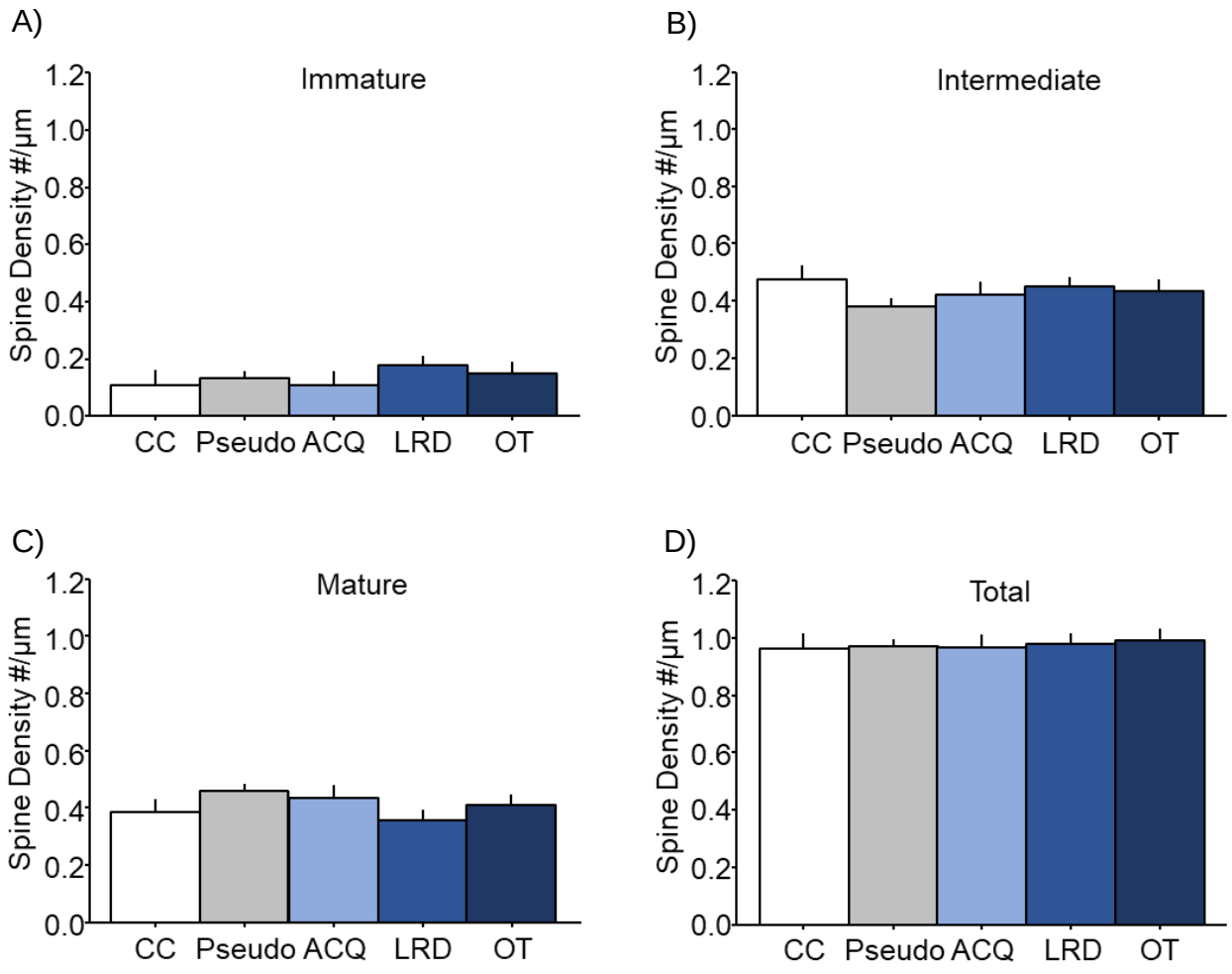

Figure 7. Fourth order basilar dendritic spine density S1 layer III pyramidal cells remains unchanged during learning of WTEB. A-D) Analyses of dendritic spine number/µm for each morphology (immature, intermediate, and mature) as well as all morphologies combined (total) revealed no significant differences between cage controls (CC), pseudo-conditioned controls (Pseudo), or trace-conditioned acquisition (ACQ), learned (LRD), or overtrained (OT) subjects.

CHAPTER II: SHANK1 is Differentially Expressed during Development in CA1 Hippocampal Neurons and Astrocytes

Abstract

Recent studies have strongly suggested a role for the synaptic scaffolding protein SHANK1 in normal synaptic structure and signaling. Global SHANK1 knockout (SHANK1-/-) mice demonstrate reduced dendritic spine density, an immature dendritic spine phenotype, and impairments in various cognitive tasks. SHANK1 overexpression is associated with increased dendritic spine size and impairments in fear conditioning. These studies suggest proper regulation of SHANK1 is crucial for appropriate synaptic structure and cognition. However, little is known regarding SHANK1's developmental expression in brain regions critical for learning. The current study quantified cell specific developmental expression of SHANK1 in the hippocampus, a brain region critically involved in various learning paradigms shown to be disrupted by SHANK1 dysregulation. Consistent with prior studies, SHANK1 was found to be strongly co-expressed with dendritic markers, with significant increased co-expression at postnatal day (PND) 15, an age associated with increased synaptogenesis in the hippocampus. Interestingly, SHANK1 was also found to be expressed in astrocytes and microglia. To our knowledge, this is the first demonstration of glial SHANK1 localization; therefore, these findings were further examined via a glial purified primary cell culture fraction using magnetic cell sorting. This additional analysis further demonstrated that SHANK1 was expressed in glial cells, supporting our immunofluorescence co-expression findings. Developmentally, astroglial SHANK1 co-expression was found to be significantly elevated at PND 5 with a reduction into adulthood, while SHANK1 microglial co-expression did not significantly change across development. These data collectively implicate a more global role for SHANK1 in mediating

normal cellular signaling in the brain. This chapter has been published in Developmental Neurobiology.

Introduction

SHANK1 is a post-synaptic scaffolding protein suggested to play a critical role in neuronal development and cognition. In support of this proposed function, SHANK1 dysregulation causes impairments in many learning and cognitive assessments (Hung et al. 2008; Sungur, Schwarting, and Wohr 2016). For example, freezing behavior both 1 hour and 24 hours following contextual fear conditioning is significantly reduced in SHANK1-/- mice compared to wild type SHANK1+/+ controls (Hung et al. 2008). Similarly, SHANK1-/- pups elicit fewer vocalizations following isolation from their mothers and littermates as well as increased self-grooming in adulthood when compared to SHANK1+/+ controls (Sungur, Schwarting, and Wohr 2016). Collectively these data suggest that proper SHANK1 regulation is critical for various typical behavioral phenotypes.

In exploring a possible mechanism by which SHANK1 mediates these behaviors, many have suggested that it can do so through direct modification of synaptic networks. Anatomical studies have found that SHANK1 is localized within the post-synaptic density (PSD) of excitatory synapses (Sheng and Kim 2000; Naisbitt et al. 1999; Tu et al. 1999) and is involved in dendritic spine modifications typically observed during neuronal development. Specifically, reductions of SHANK1 expression both *in vitro* and *in vivo* decrease dendritic spine density and result in smaller dendritic spine length and width (Grabrucker et al. 2011; Sala et al. 2001; Hung et al. 2008). Furthermore, *in vitro* SHANK1 overexpression increases dendritic length and width (Sala et al. 2001). Interestingly, these anatomical changes are consistent with dendritic spine modifications observed during development, thus further suggesting a role for SHANK1 in normal neuronal development and cognition.

Consistent with this hypothesis, studies have noted abnormal SHANK1 expression in developmental cognitive disorders such as Fragile X Mental Retardation Syndrome (FXS). FXS is the leading form of inherited mental retardation and the most prominent form of Autism. FXS is caused by the transcriptional silencing of the Fragile X Mental Retardation Protein (FMRP). Interestingly, FMRP acts as a negative regulator of SHANK1 translation via interaction with the 3' untranslated region (UTR) of SHANK1 mRNA (Zhang et al. 2014). Thus, in the absence of FMRP, as observed in FXS, SHANK1 brain protein expression is abnormally upregulated compared to controls (Schutt et al. 2009). Furthermore, consistent with SHANK1 over-expression studies, anatomical studies from a FXS mouse model and human autopsy tissue have found the syndrome to be associated with an increased density of immature dendritic spines (Grossman et al. 2010; Galvez, Gopal, and Greenough 2003; Galvez and Greenough 2005; Irwin et al. 2001). These findings, along with FXS cognitive studies and behavioral SHANK1 studies suggest a possible role for SHANK1 dysregulation in FXS behavioral and cognitive abnormalities.

Given SHANK1's importance in normal neuronal development and cognition, it is surprising that little is known regarding its developmental expression in brain regions critically involved in learning and cognition. Studies have shown that SHANK1 protein levels within the PSD increase from birth through early development followed by a slight decrease in adulthood in the cortex and cerebellum (Lim et al. 1999). However, SHANK1's developmental expression in the hippocampus, a brain region uniformly accepted as being critically involved in mediating learning and normal cognition, has not been established. The aim of the current study is to characterize the expression of SHANK1 in CA1 of the hippocampus at several developmentally

relevant time points to determine the SHANK1 expression necessary for normal hippocampal development and proper cognitive development.

Materials and Methods

Animals

Male and female C57BL/6 mice *Mus musculus* (n=15) were bred in house and kept on a 12:12 light/dark cycle with food and water available *ad libitum*. At postnatal day 5 (n=3), 15 (n=3), 25 (n=3), 35 (n=3) or 60 (n=3), mice were euthanized with a lethal dose of pentobarbital and transcardially perfused with a 0.1M phosphate buffer solution (PBS) followed by a 4% paraformaldehyde solution. Brains were collected and post-fixed in 4% paraformaldehyde for 24 hours at 4°C, and then placed in a 30% sucrose solution until sectioned. All animal procedures were performed in compliance with the Institutional Animal Care and Use Committee (IACUC) at the University of Illinois Urbana-Champaign.

Immunofluorescence

Three coronal sections (30μm) per animal were stained for SHANK1 and MAP2, GFAP or IBA-1 using a standard immunofluorescence protocol. Briefly, following a rinse in a 0.1 M phosphate-buffered saline solution (PBS, pH=7.4) the sections underwent antigen unmasking in a 0.1M citrate buffer solution (pH=6) for 25 minutes at 95°C. Sections were then blocked in 3% normal goat serum and 0.5% Triton-X in PBS followed by incubation in a primary antibody cocktail of mouse anti-SHANK1 (1:1000, Abcam, ab94576) and either rabbit anti-GFAP (1:1600, EMD Millipore, ab5804), rabbit anti-MAP2 (1:1000, EMD Millipore ab5622), or rabbit anti-IBA-1 (1:5000, Wako Pure Chemical Industries, 019-19741) for 48 hours at 4°C. The sections were then incubated in a secondary cocktail of goat anti-mouse conjugated to Alexa

Fluor 488 (1:100, Thermo Fisher Scientific, A11001) and goat anti-rabbit conjugated to Alexa Fluor 633 (1:100, Thermo Fisher Scientific, A21070) for two hours at room temperature. After a series of washes the sections were incubated in 300 nM 4',6-diamidino-2-phenylindole (DAPI) (Thermo Fisher Scientific, D1306) for 5 minutes. Excess DAPI was then rinsed off and the sections were coverslipped with ProLong Diamond mounting medium (Thermo Fisher Scientific).

Images and Analysis

Images (160.04 μm^2) of the stratum radiatum CA1 region of the hippocampus of each section were acquired using a Zeiss LSM 700 confocal microscope at 40x magnification. Z-stack images of 0.9 µm thick sections were collected and SHANK1 co-expression was assessed for each cell type. Images were then analyzed using the open source FIJI program (ImageJ extension). Individual channel fluorescence intensity and Pearson's correlation coefficients between pixel intensities of SHANK1 and each cellular marker were obtained with the Coloc 2 plugin. Sum fluorescence intensity for each antigen was also obtained from the Coloc 2 output for comparison across time-points. To calculate CA1 volume, 4-7 coronal sections spanning the hippocampus for each subject were stained with a standard Nissl protocol. Using standard non-biased stereological techniques, the area of CA1 for each section was then traced in ImageJ to obtain the section area and then used to calculate the volume for each subject [Sum ([section area * section thickness] * distance to next section)]. Total CA1 expression of each antigen was then calculated (antigen expression per unit area * CA1 volume) for each subject and compared across ages.

Astroglial Primary Cell Isolation

To examine SHANK1 expression in astrocytes, a purified astrocyte primary cell fraction was prepared. For preparing the fraction, mice (P5-P7) were decapitated and brains placed in 1x SLDS (Slice Dissection Solution) on ice until ready for the isolation process. Cells were isolated utilizing a modified version of the gentleMACS system (Miltenyi, 130-092-628) (Brooks et al. 2017; Matt, Lawson, and Johnson 2016). To guarantee a high cell count, tissue samples from 3 mice were pooled. Brains were enzymatically digested with Neural Tissue Dissociation reagents at 37ºC for 35 minutes and then passed through a 70 µm mesh to remove excess debris. The cell solution was then spun at 300 x *g* for 10 minutes. The supernatant was then removed, and subsequent steps performed at 4ºC. 30% Percoll Plus (GE Healthcare, 17-0891-01) was then utilized to remove myelin. After a 10 minute spin at 1000 x *g* cells were suspended in PEB (PBS-E + 0.5% BSA) followed by a subsequent 300 x *g* spin with resuspension in PEB. The supernatant was then removed, and cells were suspended with anti-ACSA-2 magnetic beads (Miltenyi Biotec, 130-097-678) in a MS C-Tube column (Miltenyi Biotec) in a magnetic field. All non-bound cells were then washed off with PEB and discarded. Once washed the magnetic field was turned off and the previously bound astrocytes were washed off with PEB, collected, and frozen at -80ºC.

SHANK1 Expression

To determine SHANK1 expression levels in the astrocyte enriched fraction, the sample along with a whole brain control was processed as described in (Belagodu et al. 2017). Briefly, cellular fractions were lysed, and protein concentrations estimated via bicinchonic acid assay (Thermo Scientific). Forty µg of protein for each sample in a 1:1 loading buffer (475 µl Laemmli + 25 µl βME) ratio were then loaded and run on a 4-15% electrophoresis gel (BioRad) at 150 V for 15 minutes then 200 V for 25 minutes. The gel was then transferred to a nitrocellulose membrane at

100 V for 1 hour at 4ºC. The embedded membrane was then blocked with 5% TBS-T (Tris Buffered Saline with 0.05% Tween 20) for 20 minutes followed by an overnight incubation at 4ºC with SHANK1 (1:1000, Abcam, ab94576), MAP2 (1:1000, EMD Millipore ab5622), GFAP (1:1600, EMD Millipore, ab5804) and GAPDH (1:1000, Santa Cruz sc-25778) as a loading control. Following the primary incubation, the membrane was washed and incubated with anti-mouse or anti-rabbit IgG, HRP-linked secondary antibody (1:1000, Cell Signaling, 7076S/7074S) for 2 hours prior to chemiluminescent substrate exposure for 5 minutes. Membranes were imaged via BioRad ChemiDoc Touch Gel Imaging System (BioRad). The optical densities were determined through ImageJ and relative intensity of SHANK1 was calculated by dividing its optical density with that of GAPDH.

Statistics

Significance of SHANK1 co-expression with each of the cellular markers was determined using separate one-way ANOVAs. In order to meet ANOVA assumption of normality, each Pearson's correlation coefficient was transformed into a z-score $Z_i = \frac{\left(X_i - \bar{X}\right)}{S}$ where Z_i represents the z-score of an individual correlation, X_i is the Pearson's correlation coefficient for an individual image, $\bar{X}$ is the mean Pearson's correlation coefficient for all images comparing the two fluorescence channels, and S represents the standard deviation for all images comparing the two fluorescence channels. Z-scores of SHANK1 expression with each cell type were subsequently compared with age as a between subject factor. Significant differences were further examined with a post-hoc Tukey's test controlling for multiple comparisons.

Results

SHANK1 localization

Confocal microscopic analyses yielded a classic punctuated expression for SHANK1 which was found to not co-express with DAPI (Fig. 8), suggesting an absence of nuclei expression, consistent with previous studies (Sheng and Kim 2000). SHANK1 was localized within and co-expressed with MAP2 stained processes (Fig. 9), consistent with previously reported findings and suggesting dendritic localization (Lim et al. 1999). Interestingly, upon further examination it was determined that SHANK1 was also co-expressed with GFAP, suggesting astrocytic expression (Fig. 10) and IBA-1 suggesting microglial expression (Fig. 11). To our knowledge, this is the first study demonstrating glial localization of SHANK1.

Verification of astroglial localization of SHANK1

To further verify SHANK1 glial expression a purified astroglial primary cell fraction was used with western blot analyses. This analysis found that the purified astroglial fraction stained positive for SHANK1 and GFAP; however, when probed for MAP2 no bands were observed (Fig. 12). Note, MAP2 was still absent following blot over-exposure. As a control, a whole brain sample was found to be positive for SHANK1, GFAP and MAP2. These findings demonstrate that SHANK1, consistent with our immunofluorescent analyses is expressed in astrocytes.

Developmental SHANK1 co-expression profile

Co-localization analyses of SHANK1 and DAPI demonstrated no significant main effect of age (Table 1, Fig. 13A, and Fig. S1A). Note, this analysis served as a negative control, as previous studies have demonstrated that SHANK1 is absent from neuron nuclei (Sheng and Kim 2000). Analysis of SHANK1 and MAP2 co-expression over development demonstrated a significant main effect of age ($F_{(4,10)} = 4.35$, $p = .027$). Post-hoc analyses revealed a significant increase in SHANK1/MAP2 co-expression at P15 compared to P5, 25, and 35. (Table 2, Fig. 13B, and Fig.

S1B). Examination of SHANK1 and GFAP demonstrated that there was a significant main effect of age ($F_{(4,10)} = 6.88$, $p = .0063$). Post hoc analyses revealed a significant increase in SHANK1/GFAP co-expression at P5 compared to P15, P25, and P60 (Table 3, Fig. 14A, and Fig. S1C). No significant effect of age was found with SHANK1 and IBA-1 co-expression (Table 4, Fig. 14B, and Fig. S1D)

Antigen Fluorescence Intensity and CA1 volume across Development

To determine if the developmental changes in SHANK1 co-expression were due to developmental differences in overall antigen expression, the sum fluorescence intensity for each antigen (SHANK1, MAP2, GFAP, IBA-1, and DAPI) was compared across time-points. These analyses demonstrated no significant differences per unit area across development. To account for the fact that CA1 is changing in size over development, CA1 volumetric analyses were conducted, demonstrated a significant effect of age ($F_{(4,10)} = 4.19$, $p = 0.0301$). When CA1 volume was then controlled for across development (antigen expression per unit area * CA1 volume), total CA1 expression of SHANK1 demonstrated a main effect of age ($F_{(4,10)} = 4.61$, $p = 0.0228$). Post hoc analyses (Tukey) revealed a significant increase of total CA1 SHANK1 expression from P5 to P15 ($t_{(10)} = 3.61$, $p = 0.0303$). Similarly, total CA1 expression of MAP2 demonstrated a main effect of age ($F_{(4,10)} = 3.94$, $p = 0.0357$). Post hoc analyses (Tukey) revealed a similar significant increase in total CA1 MAP2 expression from P5 to P15 ($t_{(10)} = 3.47$, $p = 0.0379$). There were trending effects of age for IBA-1 ($F_{(4,10)} = 2.95$, $p = 0.0752$), and DAPI ($F_{(4,10)} = 3.47$, $p = 0.0501$) expression with no significant main effect of age in total CA1 expression of GFAP. However, these effects were primarily driven by changes in CA1 volume over age and are thus not further discussed.

Discussion

The present study utilized confocal microscopy to examine developmental SHANK1 co-expression with various cellular markers in the hippocampus, a critical brain region for learning and memory. Consistent with numerous studies, our findings demonstrated that SHANK1 strongly co-expressed with the dendritic marker MAP2 (Lim et al. 1999; Hung et al. 2008; Heise et al. 2016; Naisbitt et al. 1999). Furthermore, our subsequent analyses demonstrated that SHANK1 MAP2 co-expression peaked at P15. Consistent with these findings anatomical studies have previously demonstrated increased dendritic spine formation from P1-P60, with most proliferation occurring from P14-P21 (Kirov, Goddard, and Harris 2004; Elibol-Can et al. 2014; Fiala et al. 1998; Faber and Haring 1999). These findings suggest a correlational role for SHANK1 in CA1 developmental spine plasticity. Furthermore, these findings along with prior SHANK1 studies suggest a critical interplay between neuronal SHANK1 expression, proper dendritic spine development, and dysregulation resulting in anatomical and cognitive impairments as observed in FXS (Hung et al. 2008; Sala et al. 2001; Galvez, Gopal, and Greenough 2003; Galvez and Greenough 2005; Irwin et al. 2001; Schutt et al. 2009; Grabrucker et al. 2011; Pick, Malumbres, and Klann 2012; Sungur, Schwarting, and Wohr 2016).

Interestingly, our confocal microscopy analyses also demonstrated that SHANK1 was co-expressed with the astrocytic marker, GFAP. These findings are in contrast to prior studies suggesting that SHANK1 is specifically localized within neurons (Lim et al. 1999; Naisbitt et al. 1999; Tu et al. 1999). It is important to note that although confocal microscopy is widely used and is an accepted method for determining co-expression of different proteins of interest, the methodology has limitations, such as laser power intensity and pinhole size, which could hinder obtaining accurate co-expression. This is especially important as SHANK1 has been shown to

bind glutamate receptors in the post-synaptic density, a neuronal region that would have close proximity to glial cells (Tu et al. 1999; Naisbitt et al. 1999; De Pitta et al. 2011). Due to these limitations, great care was taken to minimize the likelihood of these and other factors that could generate a false positive co-expression. Furthermore, given the novelty of this finding, SHANK1 expression in astrocytes was further explored using an astrocyte purified cellular preparation. Using magnetic cell sorting astrocytes were isolated from whole brain tissue and then probed for SHANK1 using western blot detection. Consistent with our confocal analyses the astrocyte sample was positive for SHANK1. Note, as a control the sample was also probed for and found to be positive for GFAP but negative for MAP2, in contrast to a whole brain sample that was positive for both. These findings collectively suggest that our confocal analyses are accurate and that SHANK1 is expressed in astrocytes.

To our knowledge, this is the first evidence of SHANK1 expression in astrocytes. SHANK1 is known for playing a key role in recruiting and scaffolding glutamate receptors within the PSD of neurons (Tu et al. 1999; Naisbitt et al. 1999). In support of our discovery of astrocytic SHANK1, astrocytes have also been shown to contain the glutamate receptors NMDA (Verkhratsky and Kirchhoff 2007), AMPA (Seifert, Zhou, and Steinhauser 1997), and mGluR (Stella et al. 1994). Thus, it is not overtly surprising that SHANK1 would also be localized to astrocytes, possibly playing a similar role in scaffolding these receptors to the membrane, a research question for a subsequent study. It is surprising that this expression was not previously discovered; however, its discovery in the current study could be due to the use of the antigen unmasking protocol used. SHANK1 is known to play a role in binding various structural proteins that could potentially mask antigen binding sites, hindering cell specific detection. To our knowledge this is the first study that used an antigen unmasking protocol for the

immunohistochemical analyses and the first to examine SHANK1 expression in an astrocyte enriched cellular population.

Our co-localization analysis of SHANK1 and GFAP revealed a developmental shift in co-expression with highest co-expression at P5. It is unlikely that these results are driven by overall developmental changes in SHANK1 or GFAP expression as no significant differences in fluorescence intensity were found for either antigen across developmental time-points. Astroglial glutamate receptors have been implicated in various developmental processes related to synaptic plasticity, including synaptogenesis (Withers et al. 2017), synapse elimination (Reemst et al. 2016), and regulation of glutamatergic signaling (De Pitta et al. 2011). Interactions between SHANK1 and glutamate receptors could be involved in any of these processes; however, further research will be needed to determine its specific role.

Co-localization was also observed between SHANK1 and IBA-1, a cellular marker for microglia. Similar to astrocytes, functional glutamate receptors have been discovered on microglia (Pocock and Kettenmann 2007), suggesting that SHANK1 may be playing a similar role in anchoring these receptors to the microglia membrane. While the specific roles for these receptors are poorly understood, microglia release many growth factors important for developmental neural outgrowth such as brain-derived neurotrophic factor (BDNF), neurotrophin-3 (NT-3), and fibroblast growth factor (FGF) (Reemst et al. 2016). Currently, it is not known if microglial glutamate receptors are involved in these processes. Furthermore, the present study found no significant developmental shift in microglial SHANK1 co-expression, suggesting that its co-expression is not developmentally regulated. However, further studies will be needed to provide insight into the specific role of SHANK1 in microglia in developmental plasticity.

Interestingly this glial SHANK1 expression could play a critical role in mediating many developmental neurological disorders. For example, the Fragile X Mental Retardation Syndrome (FXS), the leading form of inherited mental retardation and the most prominent Autism Spectrum Disorder, exhibits increased SHANK1 brain expression (Schutt et al. 2009). Anatomical FXS studies have further determined that the syndrome is associated with increased density of immature dendritic spines, which is believed to contribute to the observed cognitive abnormalities (Grossman et al. 2010; Galvez, Gopal, and Greenough 2003; Galvez and Greenough 2005). While prior studies have speculated that this increased dendritic spine density is the underlying cause for the SHANK1 overexpression, the discovery of glial SHANK1 expression provides an additional site for potential disrupted regulation facilitating FXS abnormalities. In support of this argument, FXS is also associated with increased GFAP expression, suggesting either increased astrocyte number or activity (Pacey et al. 2015). Furthermore, co-culturing FMRP knockout astrocytes with wild-type neurons results in increased dendritic spine density, consistent with that observed in FXS, while co-culturing FMRP knockout neurons with wild-type astrocytes rescues dendritic spine abnormalities (Cheng, Sourial, and Doering 2012). These studies suggest that abnormalities in FXS astrocytes are mediating the observed dendritic spine abnormalities, thus further suggesting that abnormal astrocyte SHANK1 expression in FXS could be facilitating many of the dendritic spine abnormalities that are believed to be an underlying factor for the observed cognitive impairments.

Collectively the current study demonstrates that SHANK1 is developmentally expressed in hippocampal neurons and glial cells. Although the specific role for this developmental expression pattern in these different cell types is not fully understood, the current study provides

the first developmental cell-type specific expression profile. In so doing subsequent studies can better focus on the exact role of SHANK1 in these different cells at specific time points during development. Furthermore, with such an understanding, these findings will provide additional insight into how dysregulation of SHANK1, as observed in FXS, can facilitate the observed anatomical and subsequent cognitive impairments.

Figures and Tables

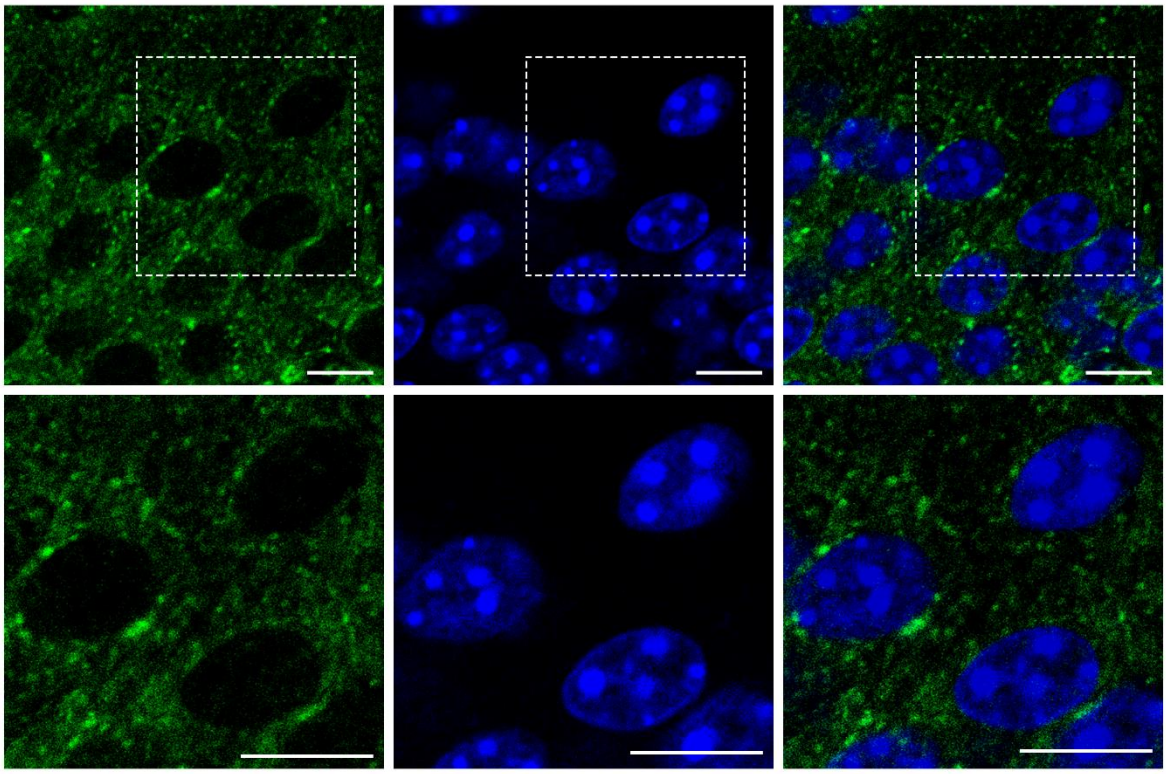

Figure 8. SHANK1 does not co-localize with the nuclear marker DAPI. Representative images obtained via fluorescence confocal microscopy of SHANK1 expression (Green: left), DAPI expression (Blue: center), and the merged images (right). Second row of images illustrate a magnified view of the delineated region in the top images. Note, there is no co-expression of the two antigens. Scale bar = 10 µm.

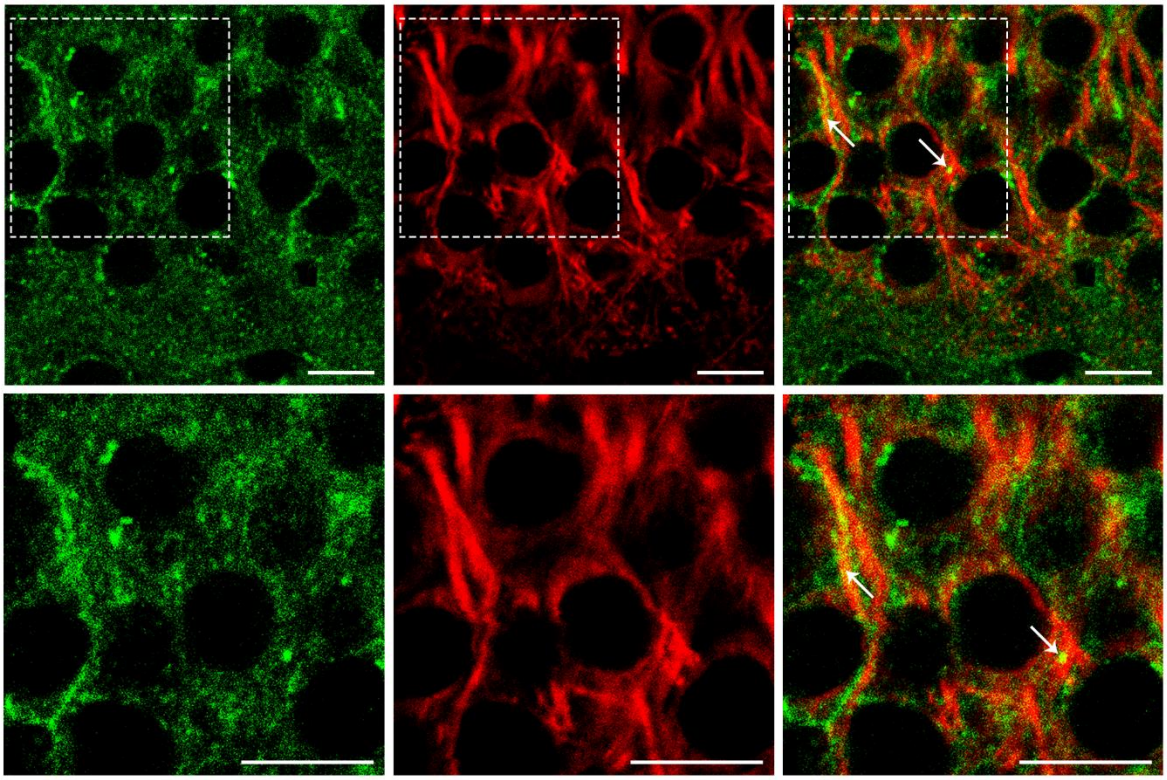

Figure 9. SHANK1 is co-localized with the dendritic marker MAP2. Representative images obtained via fluorescence confocal microscopy of SHANK1 expression (Green: left), MAP2 expression (Red: center) and the merged image (right). Second row of images illustrate a magnified view of the delineated region in the top images. Arrows mark some areas of co-expression. Scale bar = 10 µm.

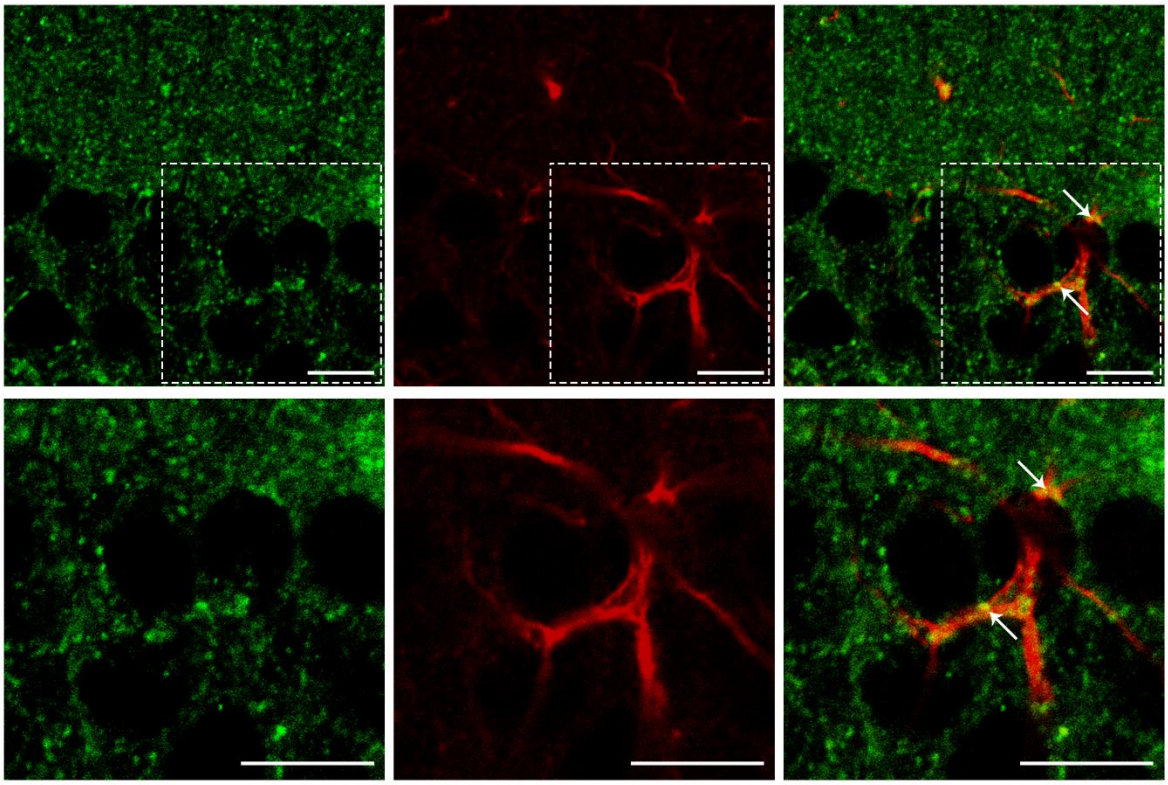

Figure 10. SHANK1 is co-localized with the astroglial marker GFAP. Representative images obtained via fluorescence confocal microscopy of SHANK1 expression (Green: left), GFAP expression (Red: center) and the merged image (right). Second row of images illustrate a magnified view of the delineated region in the top images. Arrows mark some areas of co-expression. Scale bar = 10 µm.

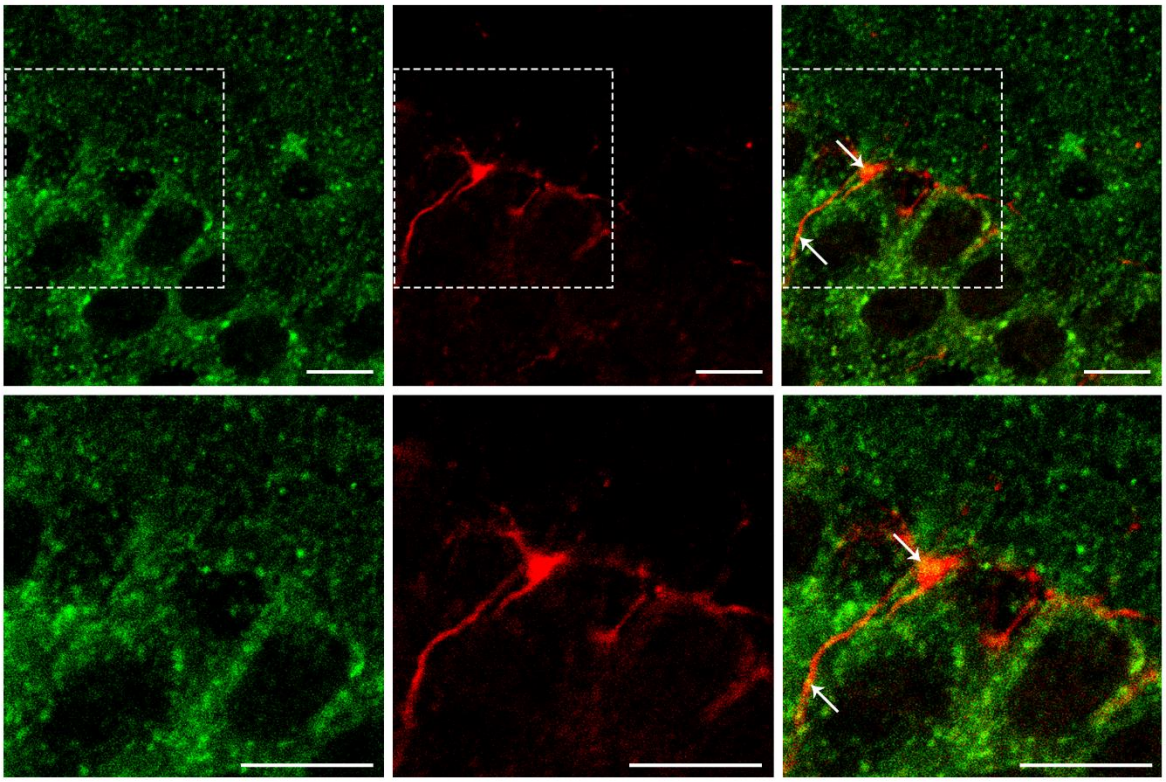

Figure 11. SHANK1 is co-localized with the microglial marker IBA-1. Representative images obtained via fluorescence confocal microscopy of SHANK1 expression (Green: left), IBA-1 expression (Red: center) and the merged image (right). Second row of images illustrate a magnified view of the delineated region in the top images. Arrows mark some areas of co-expression. Scale bar = 10 µm.

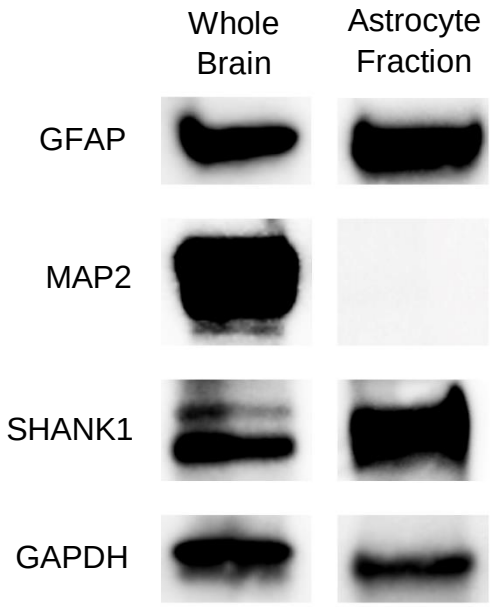

Figure 12. SHANK1 is expressed in a purified astrocyte cellular fraction. SHANK1, GFAP, MAP2 and GAPDH expression in whole brain (left) and a purified astrocyte cellular fraction (right). Note the presence of SHANK1 in both samples but the absence of MAP2 expression in the Astrocyte fraction. GAPDH served as a loading control.

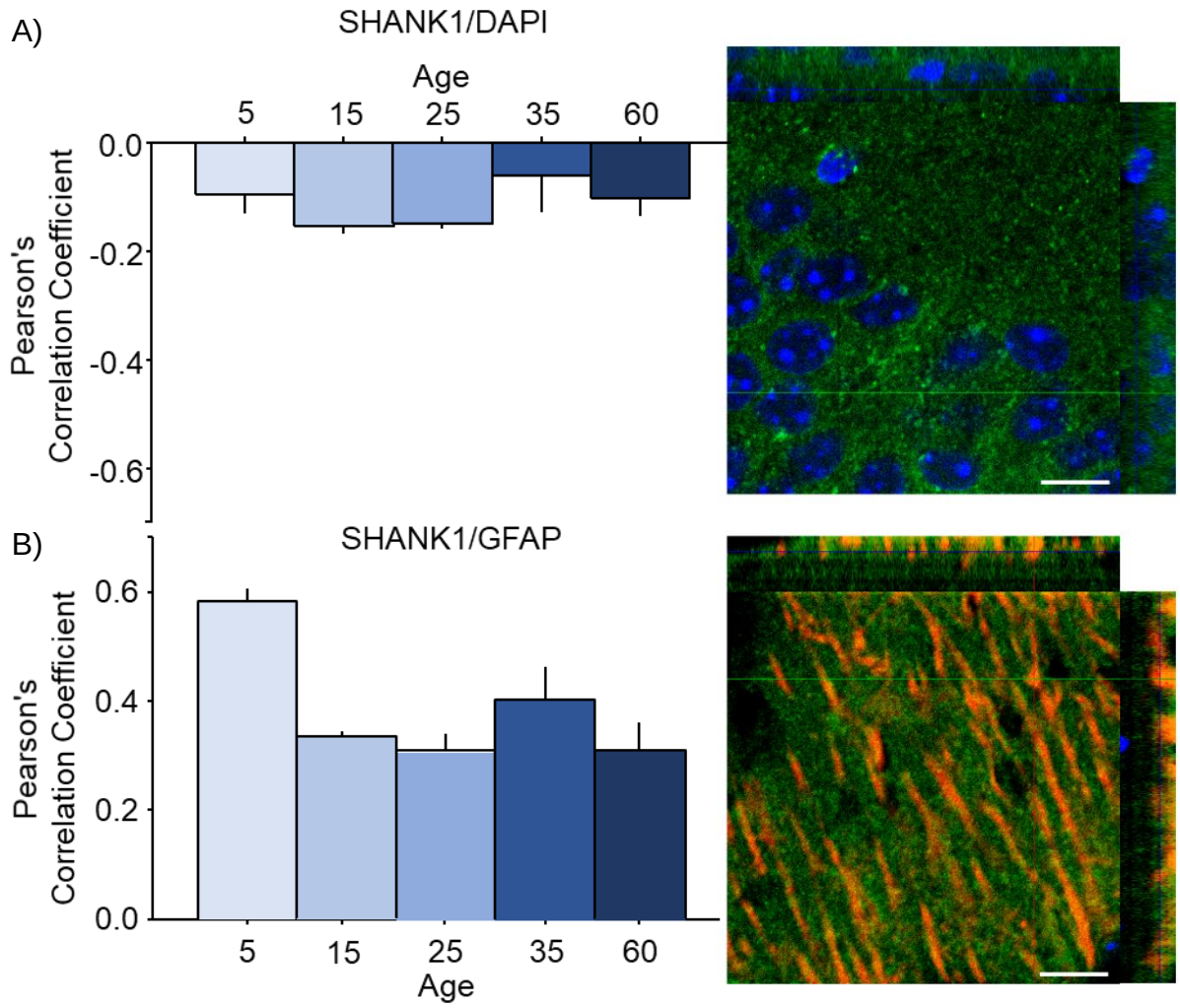

Figure 13. Relative SHANK1 co-expression in CA1 hippocampal neurons during development. A) Pearson's correlation coefficient means with standard deviations of SHANK1 and DAPI expression at P5, P15, P25, P35, and P60 (left). Representative confocal microscopy image of SHANK1 (green) and DAPI (blue) with Z plane panels (top & right). B) Pearson's correlation coefficient means with standard deviations of SHANK1 and MAP2 expression at P5, P15, P25, P35, and P60 (left). Representative confocal microscopy image of SHANK1 (green), MAP2 (red), and DAPI (blue) with Z plane panels (top & right). Scale bar = 10 µm.

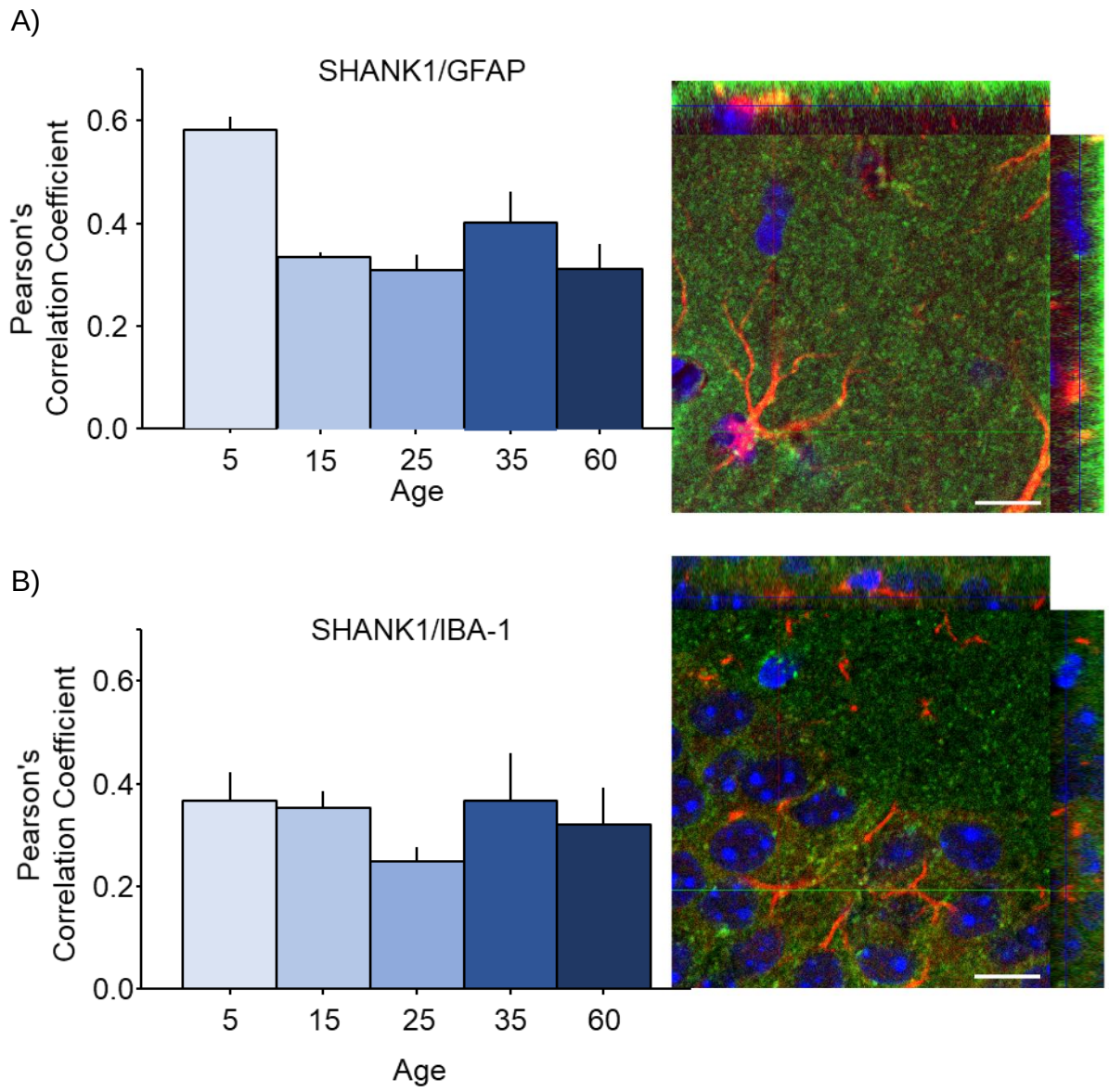

Figure 14. Relative SHANK1 co-expression in CA1 hippocampal glia during development. A) Pearson's correlation coefficient means with standard deviations of SHANK1 and GFAP expression at P5, P15, P25, P35, and P60 (left). Representative confocal microscopy image of SHANK1 (green), GFAP (red), and DAPI (blue) with Z plane panels (top & right). B) Pearson's correlation coefficient means with standard deviations of SHANK1 and IBA-1 expression at P5, P15, P25, P35, and P60 (left). Representative confocal microscopy image of SHANK1 (green), IBA-1 (red), and DAPI (blue) with Z plane panels (top & right). Scale bar = 10 µm.

	Pearson's		Z-Score		
Age	Mean	Std. dev.	Mean	Std. dev.	Sig. group
5	-0.098	0.059	-0.092	0.978	a
15	-0.154	0.026	0.143	0.532	a
25	-0.149	0.016	-0.258	0.093	a
35	-0.061	0.117	0.442	0.911	a
60	-0.104	0.053	0.007	0.309	a

Table 1. SHANK1 and DAPI developmental co-expression in CA1 of the hippocampus. Mean and standard deviation of Pearson's correlation coefficients and z-scores for SHANK1 and DAPI co-expression at each age group. Different letters in "Sig. group" columns indicate significant differences in z-scores between age groups [P5 (n = 3), P15 (n = 3), P25 (n = 3), P35 (n = 3), and P60 (n = 3)] analyzed with a one-way ANOVA. $p < 0.05$.

	Pearson's		Z-Score		
Age	Mean	Std. dev.	Mean	Std. dev.	Sig. group
5	0.184	0.005	-0.331	0.068	a
15	0.299	0.037	1.192	0.487	b
25	0.184	0.040	-0.331	0.529	a
35	0.183	0.061	-0.346	0.815	a
60	0.208	0.043	-0.021	0.572	a,b

Table 2. SHANK1 and MAP2 developmental co-expression in CA1 hippocampal neurons. Mean and standard deviation of Pearson's correlation coefficients and z-scores for SHANK1 and MAP2 co-expression at each age group. Different letters in "Sig. group" columns indicate significant differences in z-scores between age groups [P5 (n = 3), P15 (n = 3), P25 (n = 3), P35 (n = 3), and P60 (n = 3)] analyzed with a one-way ANOVA. $p < 0.05$.

	Pearson's		Z-Score		
Age	Mean	Std. dev.	Mean	Std. dev.	Sig. group
5	0.585	0.038	1.350	0.445	a
15	0.337	0.012	-0.255	0.166	b
25	0.310	0.053	-0.553	0.408	b
35	0.404	0.104	0.169	0.795	a,b
60	0.312	0.082	-0.488	0.558	b

Table 3. SHANK1 and GFAP developmental co-expression in CA1 hippocampal astrocytes. Mean and standard deviation of Pearson's correlation coefficients and z-scores for SHANK1 and GFAP co-expression at each age group. Different letters in "Sig. group" columns indicate significant differences in z-scores between age groups [P5 (n = 3), P15 (n = 3), P25 (n = 3), P35 (n = 3), and P60 (n = 3)] analyzed with a one-way ANOVA. $p < 0.05$

	Pearson's		Z-Score		
Age	Mean	Std. dev.	Mean	Std. dev.	Sig. group
5	0.367	0.095	0.223	0.717	a
15	0.352	0.055	0.113	0.421	a
25	0.249	0.047	-0.671	0.359	a
35	0.366	0.163	0.214	1.239	a
60	0.320	0.125	-0.132	0.948	a

Table 4. SHANK1 and IBA-1 developmental co-expression in CA1 hippocampal microglia. Mean and standard deviation of Pearson's correlation coefficients and z-scores for SHANK1 and IBA-1 co-expression at each age group. Different letters in "Sig. group" columns indicate significant differences in z-scores between age groups [P5 (n = 3), P15 (n = 3), P25 (n = 3), P35 (n = 3), and P60 (n = 3)] analyzed with a one-way ANOVA. $p < 0.05$

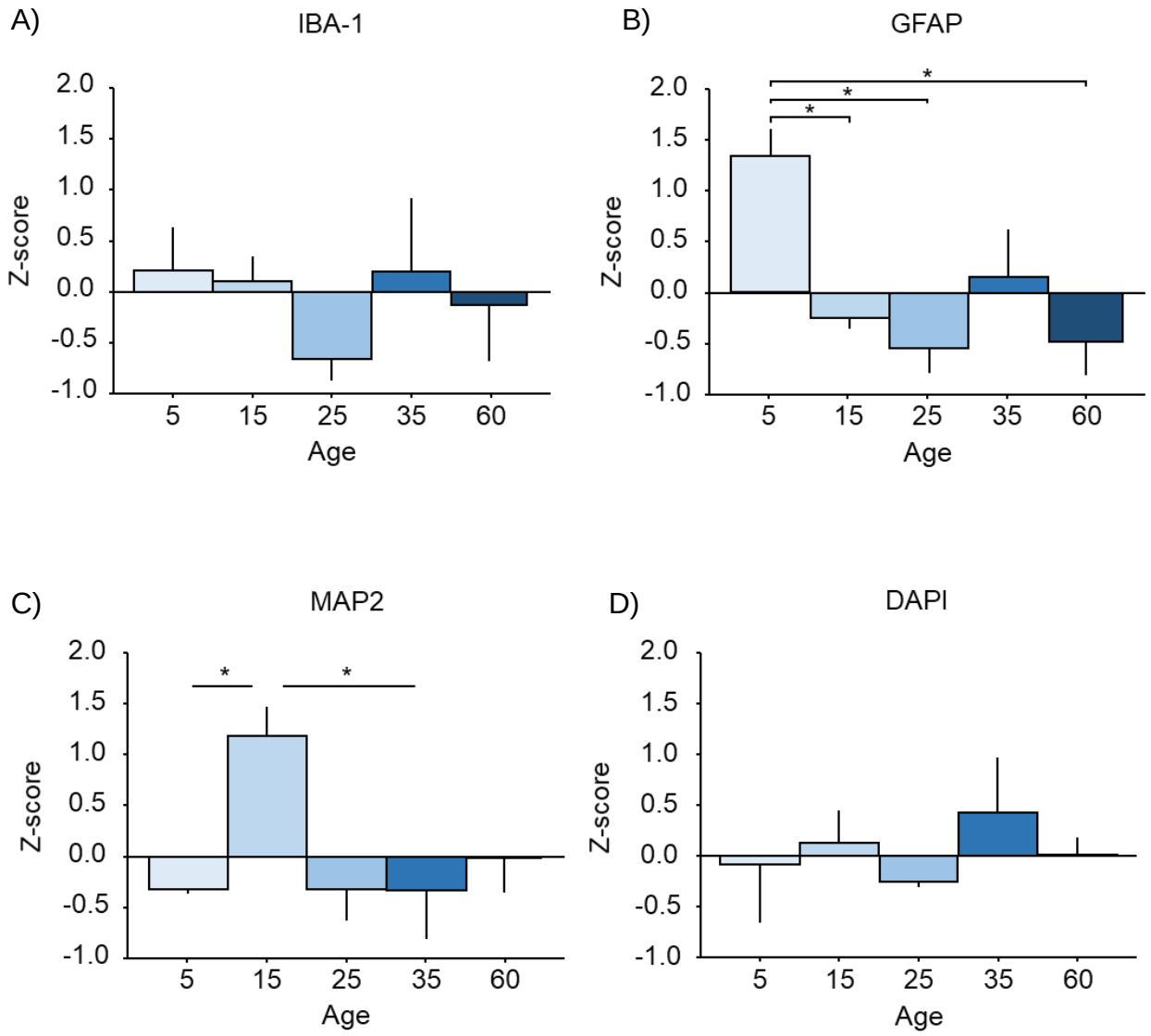

Supplementary Figure 1. Comparison of z-scores obtained from Pearson's correlation coefficients. A) – D) Z-score means with standard error of mean (S.E.M) calculated from Pearson's correlation coefficients of SHANK1 and each cellular marker (DAPI, MAP2, GFAP, and IBA-1). Statistical differences across ages [P5 (n = 3), P15 (n = 3), P25 (n = 3), P35 (n = 3), and P60 (n = 3)] were analyzed with individual one-way ANOVAs for each cellular marker. * = $p < 0.05$.

CHAPTER III: Neocortical SHANK1 regulation of forebrain dependent associative learning

Abstract

Learning-induced neocortical synaptic plasticity is a well-established mechanism mediating memory consolidation. Classic learning paradigms have been shown to elicit synaptic changes in various brain regions including the neocortex. Work from our laboratory has further suggested synaptic remodeling in primary somatosensory cortex (S1) during forebrain-dependent associative learning. While this process of dendritic spine remodeling is largely believed to contribute to memory consolidation, the underlying processes mediating this plasticity are poorly understood. Interestingly, recent studies have suggested that the synaptic scaffolding protein SHANK1 plays a critical role in this process. Increasing SHANK1 expression increases dendritic spine length and width, while decreasing SHANK1 expression reduces dendritic spine density. Furthermore, genetically knocking out SHANK1 expression impairs acquisition of various associative learning paradigms. Although these studies clearly suggest a role of SHANK1 during learning, to date there are very few studies directly examining the role of SHANK1 across a learning event in the neocortex, the most likely site of memory consolidation. To directly explore SHANK1's potential role during learning and memory, the following study set out to both examine neocortical SHANK1 expression during a learning event and determine the consequences of reducing neocortical SHANK1 expression on learning. Prior studies have explored the effects of genetically eliminating SHANK1 expression; however, these studies have the added confound of potential compensatory mechanisms contributing to any observed behavioral abnormalities. The current study found that SHANK1 expression is transiently increased during periods of learning-induced dendritic spine plasticity in the neocortex.

Furthermore, shRNA-mediated neocortical SHANK1 knockdown significantly impairs acquisition for a forebrain-dependent associative learning task (whisker trace eyeblink conditioning). Consistent with these findings, SHANK1 has been implicated in various neurological disorders. Collectively, these findings suggest a role for SHANK1 in neocortical learning-induced dendritic spine plasticity underlying learning and normal cognition; thus, providing potential insight into neurological mechanisms mediating abnormalities of impaired cognition. This chapter has been submitted for publication.

Introduction

It is well established that learning elicits neocortical synaptic plasticity, a mechanism that is widely accepted to underlie neocortical memory consolidation (Turner and Greenough 1985; Kleim et al. 1996; Knott et al. 2002; Barnes and Finnerty 2010). Consistent with this theory, our laboratory has demonstrated that acquisition of the forebrain dependent associative paradigm whisker-trace-eyeblink conditioning (WTEB) induces time- and learning-dependent neocortical dendritic spine modifications (Chau, Prakapenka, et al. 2014). WTEB is an associative learning paradigm that pairs a neutral conditioned stimulus (CS; whisker stimulation), following a stimulus-free interval, with an unconditioned stimulus (US; mild periorbital eye-shock) that elicits a behavioral response (eyeblink). This form of conditioning is both hippocampal and neocortical dependent in that pre-training lesions of either the dorsal hippocampus or primary somatosensory cortex (S1) impairs acquisition for the task (Galvez, Weible, and Disterhoft 2007; Tseng et al. 2004). Using this paradigm, our laboratory has previously demonstrated that dendritic spine density on spiny stellate neurons in layer IV of S1 increases with initial task acquisition. However, with continued training, dendritic spine density returns to pre-training levels, suggesting synaptic remodeling with learning (Chau, Prakapenka, et al. 2014).

Although learning-induced neocortical synaptic plasticity is now a widely accepted process for memory consolidation, the underlying molecular mechanisms mediating this plasticity remain largely unknown. Interestingly, recent studies have suggested that one mechanism facilitating these changes could be through modulation of the synaptic scaffolding protein, SHANK1. SHANK1 has primarily been reported to be localized within the post-synaptic density (PSD) of excitatory synapses (Sheng and Kim 2000) playing a critical role in anchoring of glutamate receptors. Studies have further shown that genetically decreasing SHANK1

expression decreases dendritic spine density (Grabrucker et al. 2011; Hung et al. 2008; Wang et al. 2011), length, and width (Hung et al. 2008). In contrast, over expressing SHANK1 alters dendritic spine morphology, causing increase in spine head length and width (Hung et al. 2008; Durand et al. 2012; Berkel et al. 2012; Sala et al. 2001). These studies suggest that learning-induced dendritic spine plasticity is mediated through altered SHANK1 expression.

Studies have further suggested that SHANK1 plays a role in normal learning and cognition. SHANK1 knockout (KO) mice are significantly impaired in their ability to recall contextual fear associations (Hung et al. 2008). Likewise, recollection of both cued and contextual fear conditioning is impaired in SHANK1 overexpressing mice (Hung et al. 2008; Pick, Malumbres, and Klann 2012). Interestingly, SHANK1 brain expression has also been shown to be significantly elevated in a mouse model of the Fragile X Mental Retardation Syndrome (FXS), the leading form of inherited mental retardation, and the most common single gene cause for Autism Spectrum Disorder (Tassone et al. 2012). These studies suggest that appropriate SHANK1 regulation plays an important role in normal learning and cognition.

Although these studies clearly suggest that proper SHANK1 regulation is critical for learning-induced synaptic remodeling necessary for memory consolidation, a role for SHANK1 during normal learning-induced synaptic plasticity has not been extensively explored. Most studies exploring SHANK1's role in learning have utilized global SHANK1 genetic KO models that have been shown to exhibit reduced dendritic spine density and size within the CA1 region of the hippocampus. Consistent with these findings, SHANK1 KO mice also exhibit reduced freezing following contextual fear conditioning and impairments in long-term retention of an eight-arm radial maze (Hung et al. 2008). However, due to possible compensatory mechanisms, it is unknown if the observed anatomical or learning abnormalities are due to abnormal

development, deficits in learning-induced adult synaptic remodeling, or abnormalities in both processes.

To better explore the role of SHANK1 in learning the following study conducted two distinct experiments. In the first experiment, an extensive analysis of SHANK1 protein levels in S1 during the associative learning paradigm WTEB was conducted. WTEB is a forebrain-dependent paradigm with a well-establish synaptic profile as discussed above. In the second experiment the behavioral effects of knocking down SHANK1 expression in S1 with a short hairpin RNA (shRNA) on WTEB acquisition was assessed. Although shRNA only reduces protein expression, this study has the advantage over traditional KO studies in that it would minimize potential developmental abnormalities or compensatory processes that would arise with congenital KOs hindering normal cognition. Our analyses found that SHANK1 protein levels were transiently increased in S1 consistent with known synaptic modifications during WTEB. In the second experiment it was further determined that shRNA-mediated SHANK1 knockdown in S1 significantly impaired acquisition for the WTEB association. These findings provide evidence for the importance of SHANK1 in normal cognition while offering further insight into potential mechanisms underlying neocortical synaptic remodeling and deepening our understanding of memory consolidation within specific learning networks.

Methods

Experiment I: Neocortical Learning-induced SHANK1 Expression

Animals

Male C57BL/6 mice, aged 3-6 months, (n = 41) were bred in house and housed with littermates until day of surgery at which time they were transferred to individual standard clear laboratory cages (12” x 12” x 12”). Mice were maintained on a 12:12 light/dark cycle with food and water

available *ad libitum*. All animal procedures were performed in compliance with the Institutional Animal Care and Use Committee (IACUC) at the University of Illinois Urbana-Champaign.

Surgery

The surgical procedure was performed as previously conducted (Galvez et al. 2009). Briefly, mice were anesthetized via intraperitoneal (IP) administration of a ketamine/xylazine cocktail (ketamine 1 mg/kg; xylazine 6 mg/kg). Once anesthetized, fur was shaved from the head and mice were secured in a stereotaxic apparatus. The scalp was cleaned with 70% alcohol followed by a betadine antiseptic scrub. Two percent lidocaine (.03 ml) was then injected under the skin at the incision site for local anesthesia. A small (~2 cm) incision was made across the midline of the head to expose the skull. A "headbolt" containing two Teflon-coated steel wires and an uncoated steel ground wire was then secured to the skull with dental cement. Coated wires were fed under the scalp to the periorbital region and the coating was removed from the contact site around the eye. The ground wire was then tightly secured to a screw inserted into the surface of the skull. Upon surgery completion, mice received an IP injection of carprofen (5 mg/ml, 0.3 ml) and were given 7-9 days to recover before start of behavioral training.

Behavioral training

Mice were trained as previously reported (Galvez et al. 2009). Briefly, conditioning was performed in standard clear laboratory cages within a large sound-attenuated chamber. Headbolts were connected to free-hanging tethers that provided whisker and periorbital stimulation as well as record eyelid closure using a custom LabView program. On the day preceding training, mice were habituated to the chamber and tether for 10 minutes. Following the habituation day, mice were exposed to daily conditioning sessions consisting of 30 conditioning trials separated by 15-

25 s intertrial intervals. Individual trials consisted of a 250 ms whisker stimulation (CS) paired with a 100 ms periorbital eyeshock (0.1 – 0.5 mA periobital square wave shock, 60 Hz, 0.5 ms pulses; US). The CS and US were temporally separated by a 250 ms stimulus-free trace interval (Fig 1A). For blink analysis a live feed from a camera on the tether focused on the eye was converted into a binary image and analyzed with the LabView program in real time as previously conducted (Loh et al 2017). Eyelid closure resulted in a change in area of the binary image. For individual mice, a threshold change in area was established for classification of conditioned responses (CRs) that corresponded to 2 standard deviations from baseline. A CR was defined as a suprathreshold deviation of area of the binary image from baseline occurring after CS onset and before US onset. For quantification of SHANK1 protein levels across WTEB, mice were randomly assigned to a trace-paired (n = 20) or pseudo-unpaired (n = 21) conditioned group. Trace-paired mice were further randomly divided into either an acquisition (ACQ, n = 8), learned, (LRD, n = 7), or over-trained (OT, n = 6; Fig 1B-E) group using previously established behavioral criteria (Chau, Prakapenka, et al. 2014). Mice in the ACQ group were trained until they exhibited three CRs in five consecutive trials. LRD mice were trained until they exhibited four CRs in five consecutive trials and OT mice were trained until they performed two consecutive days of exhibiting four CRs in five consecutive trials. Pseudo-conditioned controls were randomly yoked to each trace conditioned mouse so that they received the same number of CS and US trials but in an unpaired order to account for stimulation-induced plasticity. Cage controls (CC, n = 7) did not undergo surgery or conditioning and were collected at the same time as conditioned mice.

Quantification of SHANK1 expression during WTEB

Six evenly-spaced coronal sections (30 μm) from S1 of each animal were stained for SHANK1 using a standard immunohistochemical protocol (Chau et al. 2013). Briefly, following a rinse in 0.1 M phosphate-buffered saline (PBS, pH = 7.4) the sections underwent antigen unmasking in a 0.1 M citrate buffer solution (pH = 6) for 25 min at 95°C. Sections were then incubated in 3% normal goat serum and 0.5% Triton-X in PBS for 30 min. Sections then underwent a 15 min incubation in an avidin-biotin blocking solution (Vector Laboratories, SP-2001). Following this solution, sections were placed in mouse anti-SHANK1 (1:1000, Abcam, ab94576) antibody for 48 hours at 4°C. The sections were then washed and incubated in a biotinylated goat anti-mouse IgG secondary antibody solution (1:100, Vector Laboratories, BA-9200) for two hours at room temperature. Following a series of washes, sections were then incubated in an avidin-biotin complex (Vector Laboratories, PK-6100) for 45 min. Sections were then washed and visualized via DAB peroxidase substrate detection consisting of 0.5 mg/mL DAB, 6.95 mg/mL $(NH_4)_2Ni(SO_4)_2$, and 0.066 μL/mL H_2O_2 in tris-buffered saline (6.06 mg/mL Tris HCl and 1.39 mg/mL Tris Base in ddH_2O). Images were then acquired using an Olympus BX50 upright light microscope at 60x magnification (Fig 2B). During imaging, S1 was equally divided into three regions labeled supergranular, granular, and subgranular (Fig 2A) based on prior studies (Woolsey and Van der Loos 1970). Region-specific optical density analysis was then performed with Image J (https://imagej.nih.gov/ij/).

Statistics

Behavioral analysis was conducted with mixed model ANOVAs comparing % CR between each learning condition compared with the respective pseudo-conditioned controls across the within variable of training day. Given prior findings from our laboratory demonstrating learning-dependent dendritic spine plasticity in the granular region of S1 (Chau, Prakapenka, et al. 2014),

SHANK1 DAB expression between groups was initially examined in the granular layer with subsequent one-way ANOVAs for the other two regions. Significant differences between groups were further examined with post-hoc Tukey tests controlling for multiple comparisons.

Experiment II: shRNA-mediated Neocortical SHANK1 Knockdown

Animals

Male C57BL/6 mice, aged 3-6 months, (n = 24) were bred in house and housed with littermates until day of surgery at which time they were transferred to individual standard clear laboratory cages (12" x 12" x 12"). Mice were maintained on a 12:12 light/dark cycle with food and water available *ad libitum*. All animal procedures were performed in compliance with the Institutional Animal Care and Use Committee (IACUC) at the University of Illinois Urbana-Champaign.

Surgery

Stereotaxic headbolt surgeries were performed as outlined in Experiment I with the addition of a guide cannula for micro infusion of drugs into S1 as previously described (Loh et al. 2017). Briefly, a small craniotomy was made directly above S1 using a surgical dental drill and a 4 mm 26 gauge stainless steel guide cannula (PlasticsOne) was inserted into S1 (-.08 mm AP, 3 mm ML from bregma, and -0.5 mm DV from brain surface) contralateral to the periorbital wires. The headbolt and guide cannula were secured to the skull using dental cement. Upon completion of the surgery an obdurator was secured into the guide cannula and animals received an IP injection of carprophin (5 mg/ml, 0.3 ml) and normal saline (1 ml). Animals were then given 6-10 days to recover before shRNA lentiviral injections.

Administration of shRNA lentiviral particles

Following surgical recovery, mice were randomly assigned to receive intra-cannular injections of SHANK1 shRNA lentiviral particles (2.0 µl, Santa Cruz Biotechnology, sc-42197-V) or control shRNA lentiviral particles (2.0 µl, Santa Cruz Biotechnology, sc-108080). Injections into S1 were performed with a 33 gauge injection needle (plasticsOne) at an injection rate of 1.0 µl/min for 2 min (Hamilton 25 µl gastight syringe, Thermo Fisher Scientific; Legato 101 dual infuse only syringe pump, KD scientific). Following the injection, the needle remained inside the guide cannula for 2 min to allow for complete infusion.

Behavioral training

SHANK1 and control shRNA injected mice were trained to the LRD criterion as previously described in Experiment I. One hour following completion of the training session when they reached behavioral criterion, brains were collected for cannula localization (Histology) or verification of SHANK1 shRNA knockdown (Western Blot verification). See corresponding sections below.

Histology

Following completion of WTEB, a random subset of SHANK1 shRNA-injected mice (n = 5) and control shRNA-injected mice (n = 6) were decapitated and brains collected. Brains were post-fixed for 24 h in 4% paraformaldehyde the transferred to a 30% sucrose solution until sectioned. Sections (30 µm) were then stained with a standard Cresyl Violet staining protocol and examined on a light microscope to verify S1 cannula location.

Western blot verification of SHANK1 knockdown

A random subset of SHANK1 shRNA injected (n = 5) and control shRNA injected (n = 3) mice were used for verification of SHANK1 knockdown. For these mice, brains were removed, and

~1 mm x 1 mm samples were dissected from the injection site. Samples were immediately frozen and maintained at -80º C until western blot preparation. Sample preparation and western blot analyses were conducted as previously described (Belagodu et al. 2017). Briefly, samples were homogenized, and relative overall protein expression per sample were assessed with a bicinchoninic acid assay (Thermo Fisher Scientific). Equal amounts of protein per sample (40 µg) was then added to loading buffer (475 µL Laemmli + 25 µL βME) at a 1:1 ratio and run on a 4-15% electrophoresis gel (BioRad) at 100 V for 10 min followed by 200 V for 35 min. Separated proteins were then transferred to a nitrocellulose membrane, blocked with 5% milk in a tris-buffered saline solution containing 0.05% Tween 20 (TBS-T), and probed overnight at 4º C for SHANK1 (1:1000, Abcam, ab94576) and GAPDH (1:1000, Sata Cruz, sc-32233) as a loading control. The membrane was then washed with 5% milk in TBS-T three times for 10 min and incubated with anti-mouse or anti-rabbit IgG, HRP-linked secondary antibody (1:1000, Cell Signaling, 7076S/7074S) for 2 h. Following three 10 min TBS-T washes, the membrane was incubated for 5 min in a chemiluminescent substrate (Thermo Fisher Scientific) and imaged with a ChemiDoc Touch Gel Imaging System set for optimal detection (48.59 s) (BioRad). Protein levels (Shank1 and GAPDH) were then assessed by comparing optical density of protein bands with ImageJ. Relative GAPDH levels were compared across lanes to ensure consistent loading.

Analysis of CS and US detection threshold

To assess the possibility that shRNA-mediated SHANK1 knockdown impaired neocortical networks involved in stimuli detection, the minimum CS and US intensities to elicit an eyeblink response were measured as previously described (Loh et al. 2017). Briefly, stereotaxic headbolt surgeries were performed on subjects as mentioned above. Following a 7-9-day recovery period, subjects were randomly selected to receive either SHANK1 (n = 5) or control (n = 4) S1 shRNA-

injections. Ten days following injections, subjects were placed in a training chamber and connected to a free hanging tether as described above for CS and US delivery. To establish minimum US (shock) intensities, mice were exposed to a 0.1 mA eyeshock followed by a 0.1 mA stepwise increase until an eyeblink was detected. To establish minimum CS (whisker stimulation) intensities mice were exposed to 10% stepwise increases in whisker stimulation intensity ranging from 0 to 100% until an eyeblink was detected.

Statistics

Behavioral analysis was conducted with a one-way ANOVA comparing day to criterion between SHANK1 and control shRNA injected mice while blocking for effects between litters. Analysis for SHANK1 protein knockdown was conducted using an independent t-test comparing SHANK1 protein expression between SHANK1 and control shRNA injected mice. To test for differences in stimuli detection, two t-tests were performed comparing shock intensity thresholds and whisker intensity thresholds between SHANK1 and control shRNA-injected subjects.

Results

Experiment I: Neocortical Learning-induced SHANK1 Expression

WTEB behavioral analysis

A one-way ANOVA comparing %CRs on day of criterion between trace- and pseudo-conditioned subjects demonstrated a significant effect between groups (Fig 15; $F_{(5,37)} = 29.43$, $p < .0001$). Subsequent Tukey post-hoc analyses demonstrated that each trace-conditioned group (ACQ, LRD, and OT) exhibited significantly more %CRs on day of criterion compared to their respective yoked controls (ACQ: ($t_{(37)} = 3.41$, $p = .018$); LRD: ($t_{(37)} = 5.29$, $p < .0001$); OT: ($t_{(37)}$

= 9.38, $p < .0001$)). Furthermore, the OT group exhibited significantly more %CRs than the ACQ ($t_{(37)} = 6.52$, $p < .0001$) or LRD groups ($t_{(37)} = 3.98$, $p = .004$).

Neocortical region-specific analysis of SHANK1 during WTEB

Our analysis demonstrated a significant main effect of learning group in the granular region of S1 (Fig 16B; $F_{(4,34)} = 3.25$, $p = .023$). Further post-hoc testing demonstrated a significant 16% increase in SHANK1 expression in the LRD group compared to cage controls ($t_{(34)} = 3.28$, $p = .019$) and a significant 12% increase in the LRD group compared to pseudo controls ($t_{(34)} = 3.01$, $p = .036$). Similarly, there was a main effect of learning group in the supragranular region (Fig 16C; $F_{(4,34)} = 2.67$, $p = .049$) with post-hoc analyses demonstrating a significant 14% increase in SHANK1 expression in the LRD group compared to cage controls ($t_{(34)} = 3.20$, $p = .023$). There was also a significant effect of learning group in the subgranular region (Fig 16D; $F_{(4,33)} = 2.68$, $p = .048$). However a Tukey post-hoc analysis found that SHANK1 was only marginally increased in the LRD group compared to cage controls ($t_{(33)} = 2.60$, $p = .093$) and the LRD group compared to pseudo controls ($t_{(33)} = 2.74$, $p = .069$).

Experiment II: shRNA-mediated Neocortical SHANK1 Knockdown

SHANK1 knockdown impairs WTEB acquisition

Our behavioral assessments found that SHANK1 shRNA knockdown subjects took significantly longer (45% more days or 44% more trials) to reach behavioral criterion compared to control shRNA injected subjects. (Fig 17A-B; Days: $F_{(1,11)} = 9.18$, $p = .011$; Trials: $F_{(1,11)} = 7.09$, $p = .022$).

Verification of SHANK1 shRNA knockdown

To verify SHANK1 shRNA ability to significantly reduce SHANK1 *in vivo* expression, dissected regions of S1 in SHANK1 and control shRNA injected subjects were probed for SHANK1 protein expression using western blot analyses. SHANK1 shRNA samples had a significant (50%) reduction of SHANK1 protein levels compared to control shRNA samples (Fig 18; $F_{(1,11)} = 9.18$, $p = .011$).

Histological localization of cannula placement

Histological investigation demonstrated that all cannulas for shRNA delivery (SHANK1 and control) were localized within S1 with the most anterior placement -0.70 mm from bregma and the most posterior placement at -1.70 mm from bregma (Fig 19).

Analysis of CS and US detection

There were no significant differences in threshold shock intensities or whisker stimulation intensities between SHANK1 and control shRNA-injected subjects (Fig S2). These findings suggest that S1 SHANK1 knockdown did not impair the ability for subjects to detect conditioned or unconditioned stimuli.

Discussion

The current study explored a potential molecular process through SHANK1 expression facilitating neocortical dependent associative learning. Synaptic plasticity is a widely accepted process underlying learning and memory consolidation. Unfortunately, the molecular mechanisms underlying this plasticity remain largely unknown. Recent studies have demonstrated that SHANK1 plays a crucial role in maintaining dendritic spine number and regulating spine maturation (Grabrucker et al. 2011; Hung et al. 2008; Pick, Malumbres, and Klann 2012; Sala et al. 2001), suggesting that SHANK1 would be critically involved in learning

and memory consolidation. Consistent with this hypothesis, our findings demonstrate that SHANK1 is significantly elevated in S1 during the LRD phase of WTEB acquisition. Interestingly our findings also demonstrated that this increase in SHANK1 expression is transient as expression returns to preconditioning levels by the OT phase.

Prior studies from our laboratory have demonstrated that spine density in S1 also exhibits a transient increase during WTEB (Chau, Prakapenka, et al. 2014) suggesting that forebrain-dependent associative learning results in neocortical synaptic reorganization. These findings along with prior studies of SHANK1 regulation of dendritic spine properties and those from the current study further suggest a role for neocortical SHANK1 during this process.

Interestingly, our prior anatomical study found that dendritic spine density increased during task acquisition, a behavioral time-point where no significant changes in SHANK1 neocortical expression was observed (Fig 16). These findings further suggest that SHANK1 expression is not simply mediating increases in synaptic number, but rather contributing to other synaptic process, such as synaptic remodeling. Consistent with this hypothesis, previous studies have demonstrated that SHANK1 over-expression in CA1 neuronal cultures does not increase synaptic density but rather increases dendritic spine length and width (Grabrucker et al. 2011; Sala et al. 2001). Thus, further suggesting that our observed increase in SHANK1 expression is facilitating synaptic maturation and not driving synapse number.

In an attempt to further explore the role for SHANK1 with learning our subsequent studies explored the behavioral consequences of virally knocking down SHANK1 neocortical expression. Prior studies have demonstrated that global congenital dysregulation of SHANK1 reduces freezing behavior during both contextual and cued associative fear learning (Hung et al. 2008; Pick, Malumbres, and Klann 2012), suggesting that appropriate SHANK1 expression is

critical for normal associative learning. However, these global KO studies have the confounding issue of potential compensatory mechanisms causing behavioral deficits independent of the reduced SHANK1 expression. In the current study a viral shRNA was used to reduce SHANK1 expression within S1, thus eliminating potential long-term compensatory mechanisms and the effects of altered SHANK1 expression in other brain regions. Our findings demonstrated that knocking down SHANK1 within S1 significantly increased the number of days or behavioral trials needed to learn the association (Fig 17). In conjunction with the above experiment, these data suggest that SHANK1-mediated plasticity within the neocortex is a likely mechanism for neocortical dependent associative learning. To date, the present study is the first to demonstrate an importance for neocortical SHANK1 during learning in adult subjects and provides further support for SHANK1 in learning-induced structural plasticity mediating learning and memory consolidation.

It is generally accepted that the importance of SHANK1 in normal synaptic plasticity and cognitive functioning is linked to its role in scaffolding glutamate receptors to the cellular membrane of the PSD, thus establishing appropriate synaptic transmission (Lim et al. 1999; Hung et al. 2008; Sheng and Kim 2000). SHANK1 is comprised of several protein binding sites allowing for multiple protein-protein interactions. These domains include an SRC Homology 3 (SH3) domain, PSD-95/Dlg/ZO-1 (PDZ) domain, sterile alpha motif (SAM) domain, proline-rich region, as well as multiple ankyrin repeats (Lim et al. 1999; Sheng and Kim 2000). The SH3 region binds directly to GRIP that binds AMPARs, forming an AMPAR/GRIP/SHANK1 complex. Similarly, the SHANK1 PDZ domain forms a complex with both PSD-95 that binds to NMDARs, and the proline-rich region of Homer that binds mGluRs (Tu et al. 1999; Naisbitt et al. 1999; Lim et al. 1999). While SHANK1's involvement in construction of viable glutamate

receptor complexes is a widely supported functional role in normal cognition, few experiments have studied it directly. In CA1 hippocampal sections, amplitude and frequency of mini excitatory post synaptic currents (mEPSCs) are reduced in sections from SHANK1$^{-/-}$ KO mice compared to SHANK1$^{+/+}$ wildtype controls, but long-term potentiation (LTP) and long-term depression (LTD) do not differ between SHANK1$^{-/-}$ and SHANK1$^{+/+}$ sections (Hung et al. 2008). Additionally, hippocampal slice preparations from SHANK1$^{-/-}$ mice demonstrate reduced frequency of mini inhibitory post synaptic currents (mIPSCs) compared to SHANK1$^{+/+}$ controls. Collectively these studies suggest appropriate scaffolding of glutamate receptors by SHANK1 is a likely mechanism for appropriate balance of excitatory and inhibitory synaptic transmission crucial for normal cognition.

Interestingly in addition to its role at the synapse, recent studies have demonstrated that SHANK1 is not exclusively localized to the PSD. Recent studies have demonstrated that SHANK1 is also localized to axon terminals (Halbedl et al. 2016). Furthermore, an in vivo developmental analysis of SHANK1 hippocampal expression from our laboratory further demonstrated that SHANK1 is localized to astrocytes and microglia (Collins et al. 2017). Unfortunately, the specific role for SHANK1 at these non-PSD sites is largely underexplored, making any interpretations towards the findings of this study and its role in learning and memory difficult. However, as we move forward with understanding the roles for SHANK1 in the brain, it is important to also keep in mind how its specific function can change depending on cell type and location. We should also note that the lentivirus used for shRNA delivery in the current study would infect both neurons and glial cells. Furthermore, there is a growing literature outlining the importance of glia/neuron interactions in maintenance of synaptic plasticity, and cognition (Tay et al. 2017). Thus, the findings from the current study could be due to a reduction

in neuronal SHANK1, glial SHANK1 or both neuronal and glial SHANK1 expression. Subsequent studies with specific glial and/or neuronal SHANK1 reductions would be needed to further address this issue and explore the cell type specific roles for SHANK1 with learning.

Many studies have suggested that SHANK1 plays an important role in mediating learning-induced cognition; however, until now a direct examination of this hypothesis has been lacking. The current study provides substantial evidence that SHANK1 is critically involved in proper neocortical dependent cognition. In so doing, these findings provide further evidence for a potential mechanism mediating neocortical synaptic remodeling, thus underlying neocortical dependent learning and memory. As more such molecular players become apparent, we will gain a better understanding of how the brain consolidates information for later retrieval; thus, potentially providing insight into how to alleviate abnormalities in these processes that contribute to various neurological disorders.

Figures

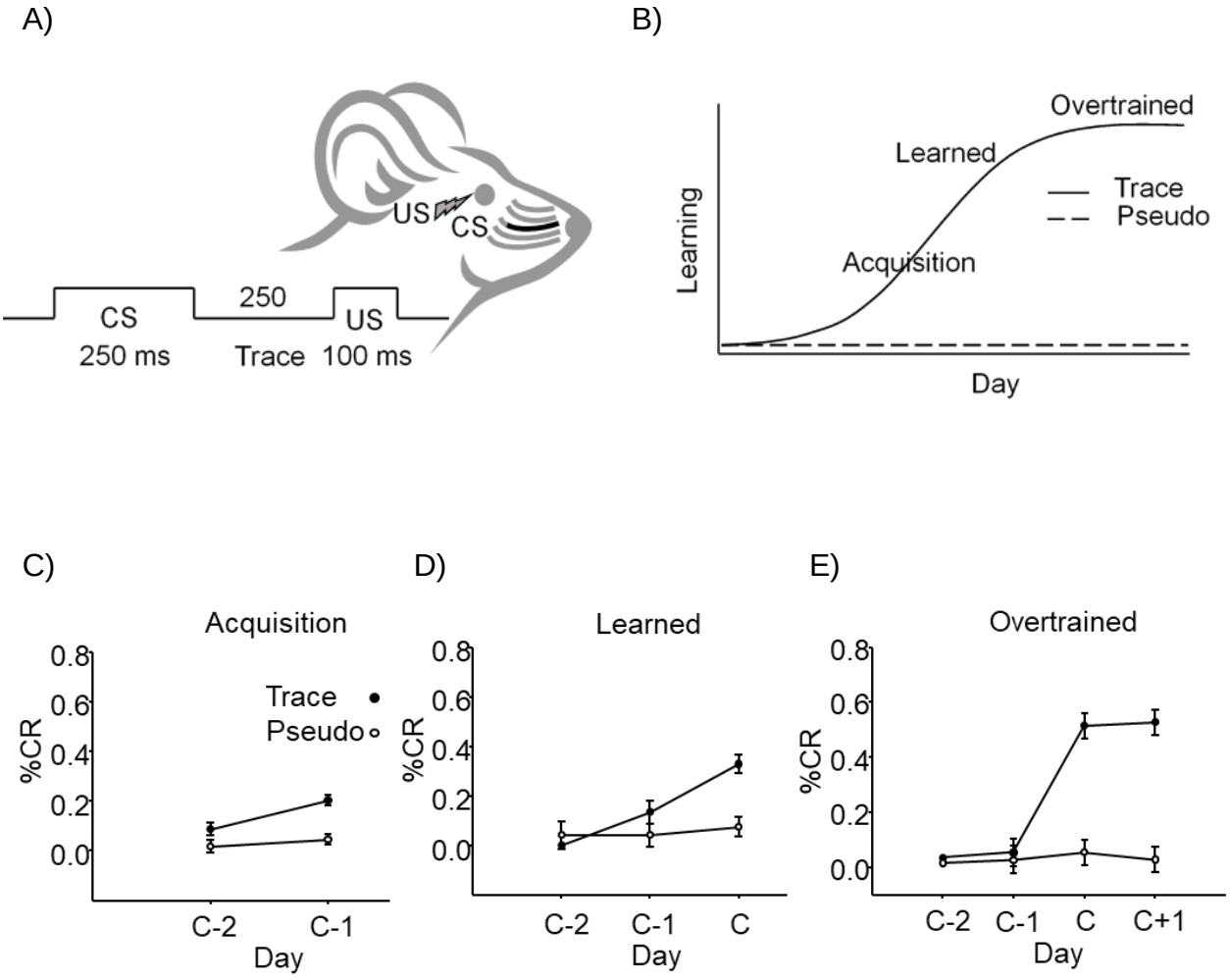

Figure 15. Behavioral analysis of neocortical-dependent whisker-trace-eyblink conditioning (WTEB). A) Schematic of temporal CS-US pairing during WTEB. Whisker stimulation (CS, 250 ms) is paired with a mild periorbital eye shock (US, 100 ms) following a stimulus free interval (trace, 250 ms). B) Theoretical WTEB learning curve demonstrating an increase in learning as a function of training comparing trace and pseudo conditioned subjects with the theoretical points for each learning time-point (Acquisition, Learned, Overtrained). C-E) WTEB performance comparing trace and pseudo conditioned subjects for each learning time-point. Note: Day C represents day of criterion for the Learned group.

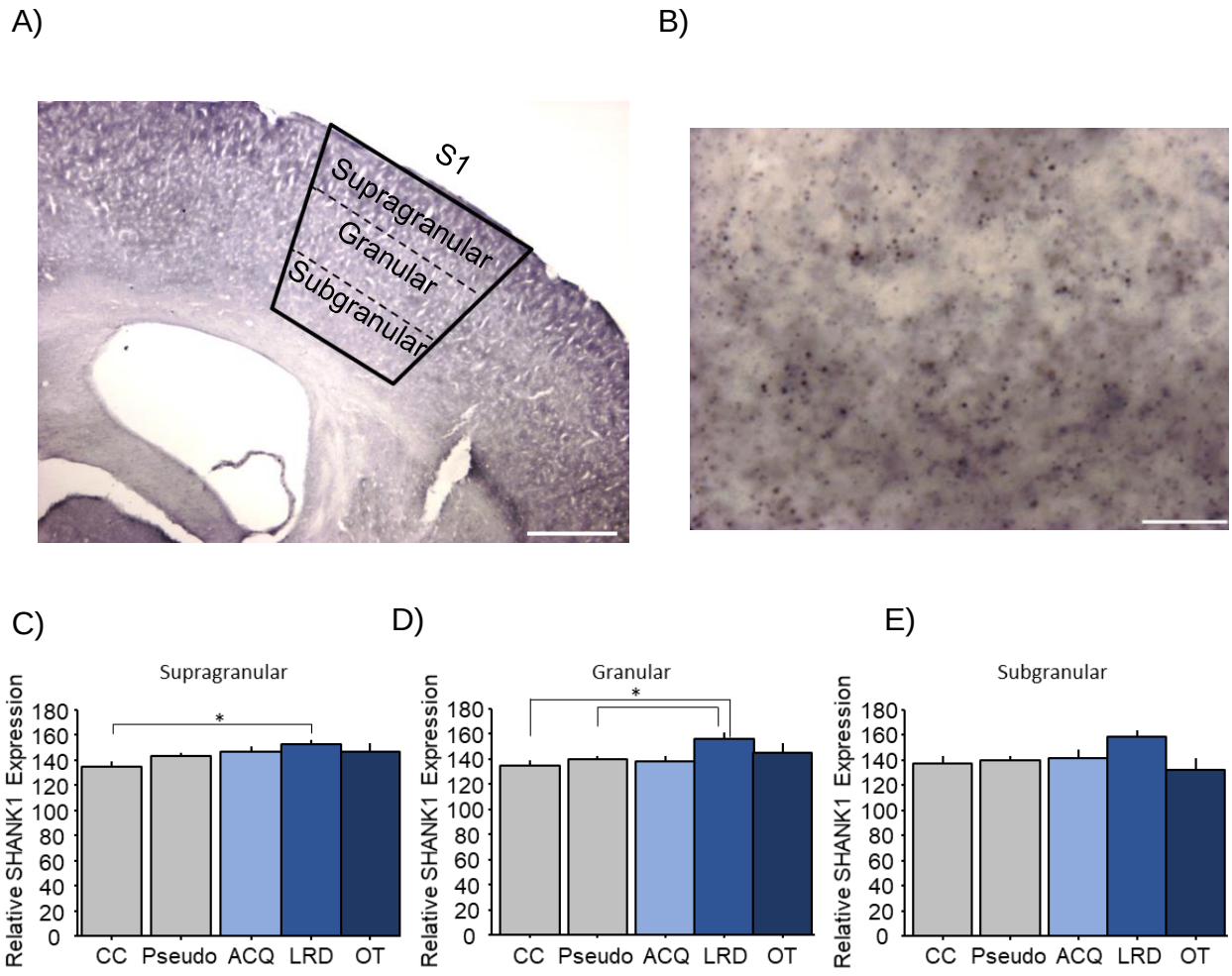

Figure 16. WTEB transiently increases primary somatosensory neocortical SHANK1 expression. Histological SHANK1 stained coronal section delineating S1 and the specific neocortical regions (Supragranular, Granular, and Subgranular) for region specific SHANK1 analysis. Scale bar = 500µm**.** B) Representative S1 SHANK1 protein expression (60x magnification). Note punctate SHANK1 expression pattern, consistent with that observed from other studies. Scale bar = 20µm. C-E) SHANK1 is increased in subjects trained to the LRD criterion in the supragranular, and granular regions of S1. * = $p < 0.05$.

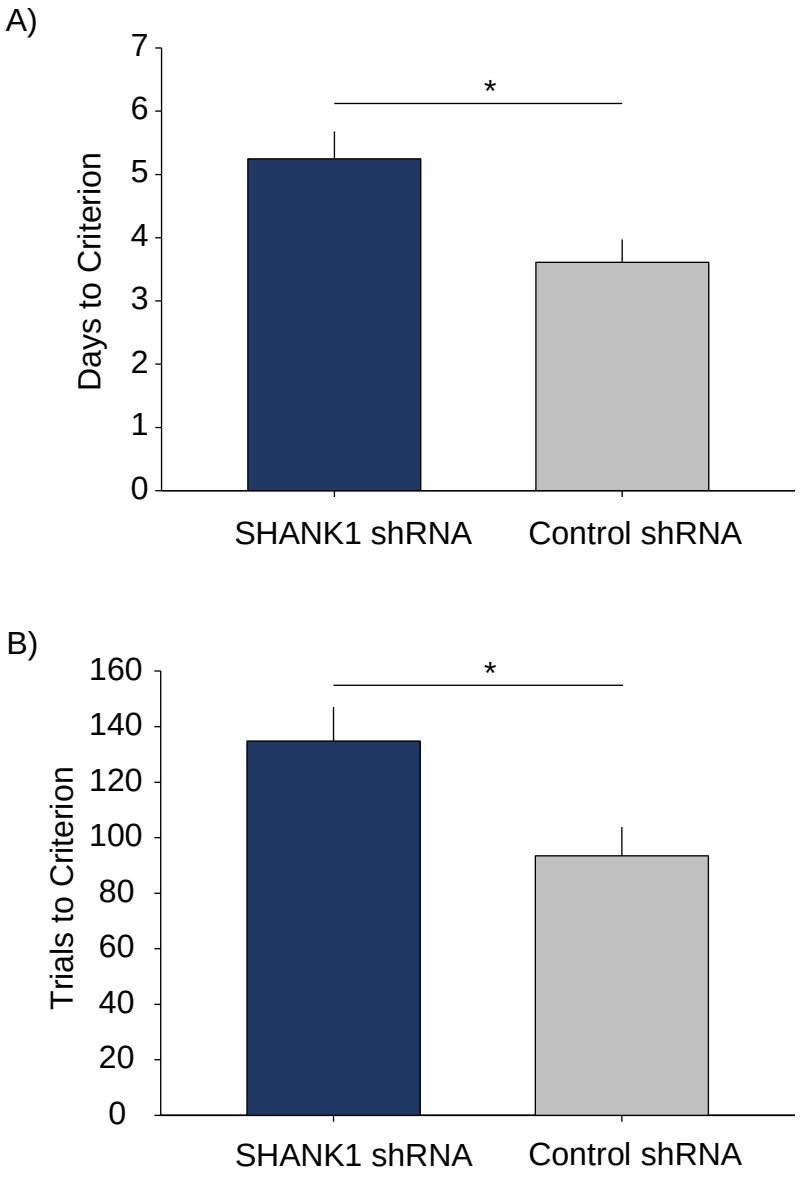

Figure 17. S1 shRNA-mediated SHANK1 knockdown significantly impairs acquisition of WTEB. A-B) Subjects injected with SHANK1 shRNA took significantly more days (45%) and trials (44%) to reach criterion compared to control shRNA injected subjects. * = $p < 0.05$.

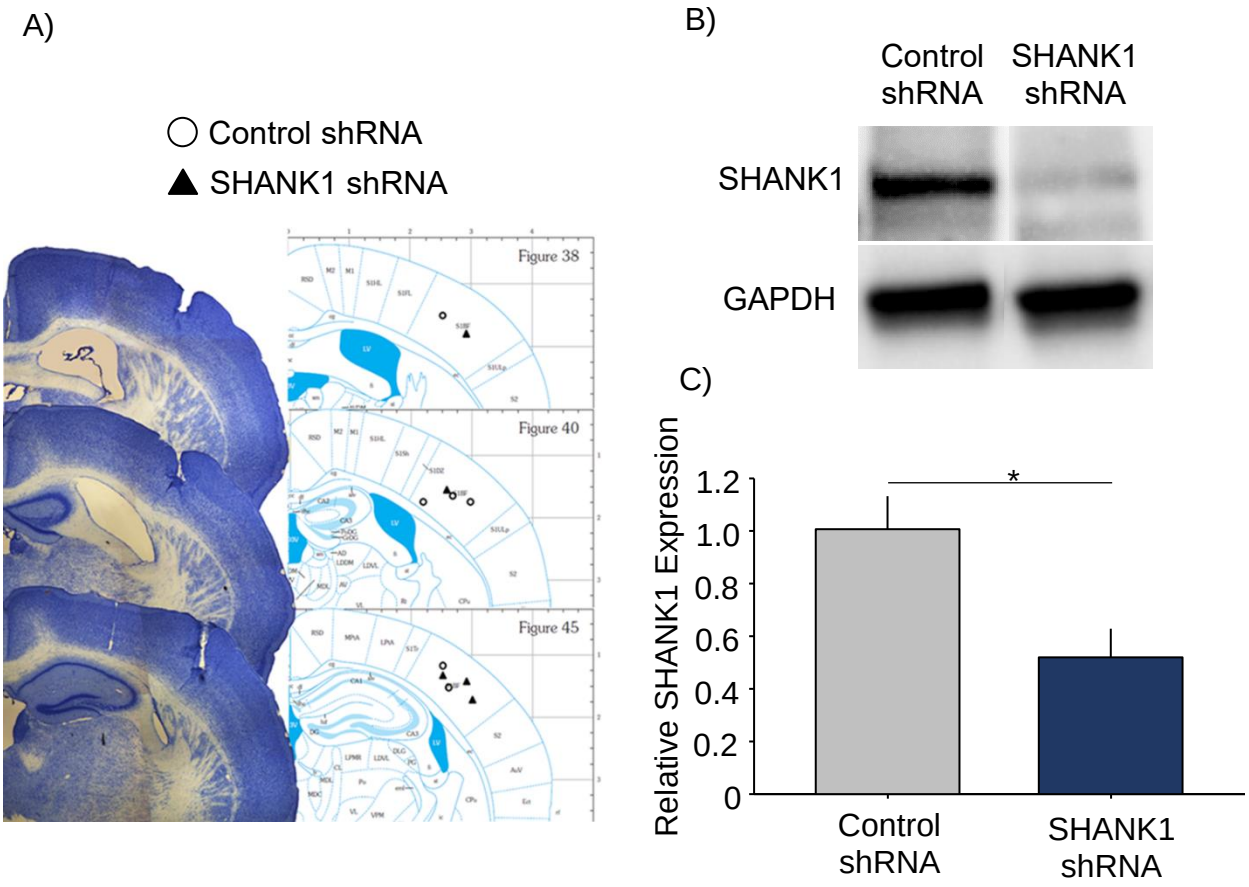

Figure 18. SHANK1 shRNA in primary somatosensory cortex significantly reduces SHANK1 expression. A) Cannula placement of control and SHANK1 shRNA injected subjects. B) Representative western blot comparing SHANK1 and GAPDH levels between control and SHANK1 shRNA injected subjects. C) SHANK1 shRNA injected subjects demonstrated a 50 percent reduction in S1 SHANK1 protein levels compared to control shRNA injected subjects. * = $p < 0.05$.

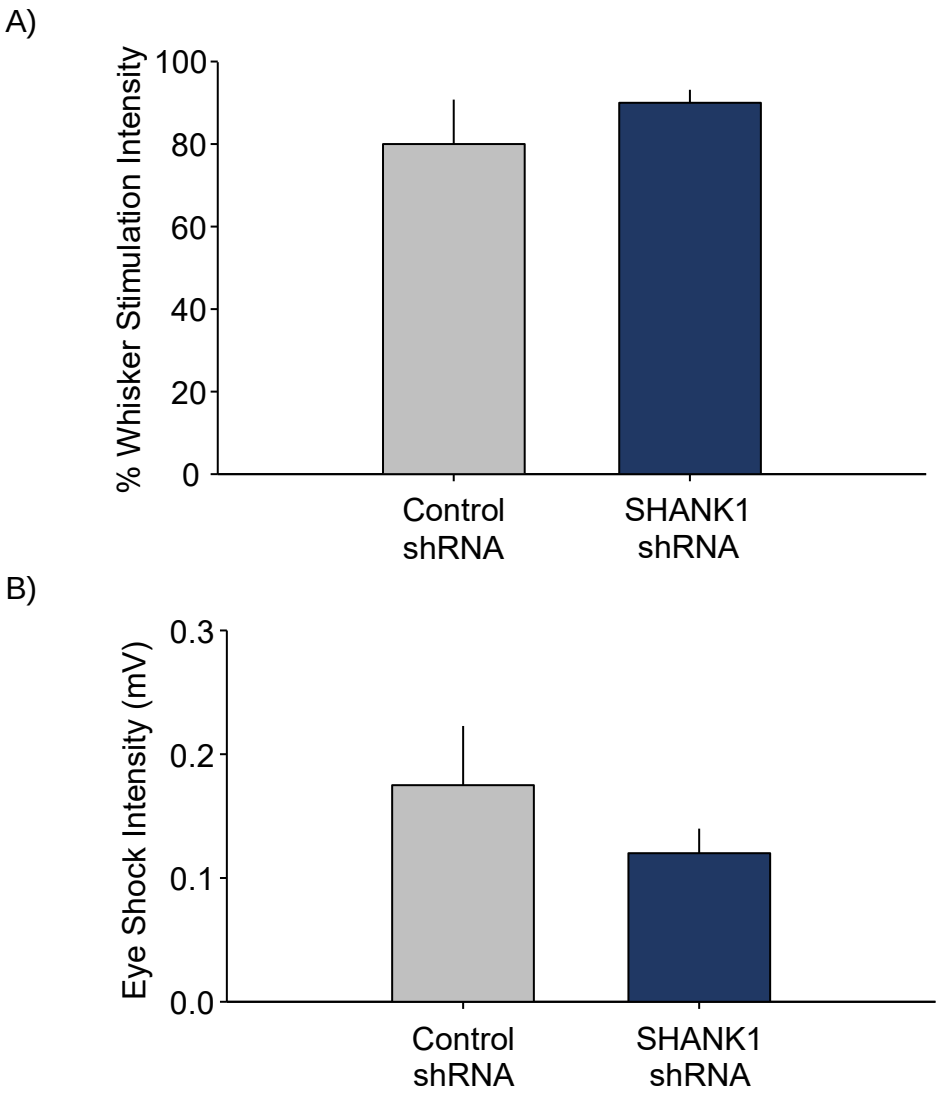

Supplementary Figure 2. Whisker stimulation and eye shock intensity threshold is similar between control and SHANK1 shRNA injected subjects. A) Whisker stimulation intensity threshold to elicit an eyeblink comparing control and SHANK1 injected subjects. B) Eye shock intensity threshold to elicit an eyeblink comparing control and SHANK1 injected subjects.

DISCUSSION

The neocortex has been well-established as a likely site for long-term memory storage which is believed to be largely driven through changes in synaptic connections. For example, many classic studies have demonstrated increases in neocortical synapse number after a learning experience (Turner and Greenough 1985; Knott et al. 2002; Kleim et al. 1996). However, it is generally accepted that this learning-induced increase in dendritic synapse density is transient and with memory consolidation results in a remodeling of synaptic networks (Barnes and Finnerty 2010; Bailey, Kandel, and Harris 2015; De Roo et al. 2008). In support of this, our laboratory has demonstrated a transient increase in dendritic spines on layer IV spiny stellate cells within primary somatosensory cortex during associative whisker-trace-eyeblink-conditioning (WTEB), suggesting dendritic spine remodeling with associative learning (Chau, Prakapenka, et al. 2014). While synaptic remodeling is widely believed to play a crucial role in memory consolidation, the underlying molecular mechanisms remain largely unknown. In exploring possible molecules mediating this plasticity, studies have recently suggested SHANK1 as a likely candidate. SHANK1 is a scaffolding protein that has primarily been shown to bind glutamate receptors to the post synaptic density of excitatory neuronal synapses (Lim et al. 1999; Sheng and Kim 2000). Interestingly, SHANK1 overexpression leads to increased dendritic spine length and width, while reduction in SHANK1 expression leads to smaller dendritic spines and reduced dendritic spine density in vitro and in vivo (Sala et al. 2001; Hung et al. 2008; Grabrucker et al. 2011). Furthermore, SHANK1 knockout mice have been shown to exhibit impaired learning and cognition (Hung et al. 2008). The studies outlined in the above thesis expand upon these previous studies, suggesting a more global role of SHANK1 expression in the remodeling of synaptic networks during memory consolidation.

While prior studies suggest proper SHANK1 regulation is critical for learning-induced synaptic plasticity and memory formation, currently all studies associating SHANK1 dysfunction with memory impairments have used global SHANK1 knockouts (KOs), thus it is unknown if learning abnormalities in these studies are due to abnormal development, deficits in learning-induced adult synaptic remodeling, or abnormalities in both processes (Hung et al. 2008). To explore SHANK1 involvement with learning our initial studies explored SHANK1 expression during learning. These studies found that SHANK1 expression peaked in S1 during periods of synaptic remodeling. Interestingly, our analyses did not find a significant change in SHANK1 expression with learning in the subgranular region, a neocortical region where we did not find any anatomical dendritic spine changes. However, SHANK1 expression was found to change in the supragranular region, although no anatomical dendritic spine changes were detected in this region. Although these finding may seem contrary to SHANK1 involvement in learning and memory, increases in SHANK1 levels have been shown to increase dendritic spine length and width, suggesting a role for SHANK1 in structural modification of dendritic spines (Sala et al. 2001). Following these analyses, we subsequently demonstrated that reducing SHANK1 expression within S1 using viral shRNA, thus eliminating potential long-term compensatory mechanisms and the effects of altered SHANK1 expression in other brain regions, significantly impaired acquisition for the learned association. In conjunction with the above experiment, these data suggest that SHANK1-mediated plasticity within the neocortex is a likely mechanism for neocortical dependent associative learning.

Although prior studies suggest that the most likely role for SHANK1 with neocortical learning is through modulation of postsynaptic glutamate receptors, our studies have expanded upon this assumption, suggesting glial SHANK1 involvement in this process. Our analyses

demonstrated SHANK1 expression in astrocytes and microglia as well as neurons. These analyses further demonstrated that neuronal and glial SHANK1 expression is regulated during different periods of neuronal development and synaptic plasticity. Given SHANK1's importance in normal synaptic plasticity and its role as a master scaffolding protein for glutamate receptors, it is surprising that previous studies did not explore SHANK1 expression in glial cells, which have been shown to express functional glutamate receptors. Our studies confirm glial SHANK1 expression and expand upon our current understanding of the role for SHANK1.

Collectively, these studies have begun to outline a more global role for SHANK1 in processes involved in neocortical learning-induced plasticity and memory consolidation. Historical studies have suggested a role for SHANK1 in appropriate learning-induced synaptic remodeling through incorporating and binding glutamate receptors to the PSD during memory formation. However, our studies have expanded upon this view, suggesting that SHANK1 may also play a non-neuronal role in this process. While the specific mechanisms underlying this process are currently unknown, functional glutamate receptors are expressed in astrocytes and microglia which have been implicated in various mechanisms related to synaptic plasticity, including synaptogenesis (Withers et al., 2017), synapse elimination (Reemst et al., 2016), and regulation of glutamatergic signaling (De Pitta et al., 2011). It is important to note that the shRNA knockdown study conducted in this thesis could have reduced SHANK1 levels in neurons as well as glial cells. Therefore, it is unclear whether the role for SHANK1 in synaptic processes mediating memory formation are neuronal or glial. Future research will need to focus on utilizing SHANK1 shRNA constructs with glial or neuronal promoters to explore this further.

Given the role for SHANK1 in synaptic plasticity in learning, it is not surprising that SHANK1 dysregulation has been liked to several neurological disorders including FXS (Schutt

et al. 2009), ASD (Sato et al. 2012), and schizophrenia (Lennertz et al. 2012). Similarly, glial abnormalities have been associated with FXS and ASD which may be partially influenced by abnormal SHANK1 expression (Edmonson, Ziats, and Rennert 2014; Pacey et al. 2015; Higashimori et al. 2016). Therefore, it is important for future research with these disorders to better elucidate glial and neuronal mechanisms mediated by SHANK1. These studies will not only provide a more complete picture of the structural processes mediating learning but will also provide insight to effective therapeutic targets for various neurological disorders with aberrant synaptic plasticity.

REFERENCES

Alvarez, V. A., and B. L. Sabatini. 2007. 'Anatomical and physiological plasticity of dendritic spines', *Annu Rev Neurosci*, 30: 79-97.

Bailey, C. H., E. R. Kandel, and K. M. Harris. 2015. 'Structural Components of Synaptic Plasticity and Memory Consolidation', *Cold Spring Harb Perspect Biol*, 7: a021758.

Bakin, J. S., D. A. South, and N. M. Weinberger. 1996. 'Induction of receptive field plasticity in the auditory cortex of the guinea pig during instrumental avoidance conditioning', *Behav Neurosci*, 110: 905-13.

Barnes, S. J., and G. T. Finnerty. 2010. 'Sensory experience and cortical rewiring', *Neuroscientist*, 16: 186-98.

Belagodu, A. P., L. Zendeli, B. J. Slater, and R. Galvez. 2017. 'Blocking elevated VEGF-A attenuates non-vasculature Fragile X syndrome abnormalities', *Dev Neurobiol*, 77: 14-25.

Berkel, S., W. Tang, M. Trevino, M. Vogt, H. A. Obenhaus, P. Gass, S. W. Scherer, R. Sprengel, G. Schratt, and G. A. Rappold. 2012. 'Inherited and de novo SHANK2 variants associated with autism spectrum disorder impair neuronal morphogenesis and physiology', *Hum Mol Genet*, 21: 344-57.

Bernardo, K. L., and T. A. Woolsey. 1987. 'Axonal trajectories between mouse somatosensory thalamus and cortex', *J Comp Neurol*, 258: 542-64.

Betancur, C., and J. D. Buxbaum. 2013. 'SHANK3 haploinsufficiency: a "common" but underdiagnosed highly penetrant monogenic cause of autism spectrum disorders', *Mol Autism*, 4: 17.

Bockers, T. M., M. Segger-Junius, P. Iglauer, J. Bockmann, E. D. Gundelfinger, M. R. Kreutz, D. Richter, S. Kindler, and H. J. Kreienkamp. 2004. 'Differential expression and dendritic

transcript localization of Shank family members: identification of a dendritic targeting element in the 3' untranslated region of Shank1 mRNA', *Mol Cell Neurosci*, 26: 182-90.

Boeckers, T. M., M. R. Kreutz, C. Winter, W. Zuschratter, K. H. Smalla, L. Sanmarti-Vila, H. Wex, K. Langnaese, J. Bockmann, C. C. Garner, and E. D. Gundelfinger. 1999. 'Proline-rich synapse-associated protein-1/cortactin binding protein 1 (ProSAP1/CortBP1) is a PDZ-domain protein highly enriched in the postsynaptic density', *J Neurosci*, 19: 6506-18.

Bourne, J. N., and K. M. Harris. 2011. 'Coordination of size and number of excitatory and inhibitory synapses results in a balanced structural plasticity along mature hippocampal CA1 dendrites during LTP', *Hippocampus*, 21: 354-73.

Brooks, A. K., T. M. Janda, M. A. Lawson, J. L. Rytych, R. A. Smith, C. Ocampo-Solis, and R. H. McCusker. 2017. 'Desipramine decreases expression of human and murine indoleamine-2,3-dioxygenases', *Brain Behav Immun*, 62: 219-29.

Brooks, W. J., T. L. Petit, J. C. LeBoutillier, and R. Lo. 1991. 'Rapid alteration of synaptic number and postsynaptic thickening length by NMDA: an electron microscopic study in the occipital cortex of postnatal rats', *Synapse*, 8: 41-8.

Chau, L. S., O. Akhtar, V. Mohan, A. Kondilis, and R. Galvez. 2014. 'Rapid adult experience-dependent anatomical plasticity in layer IV of primary somatosensory cortex', *Brain Res*, 1543: 93-100.

Chau, L. S., A. Prakapenka, S. A. Fleming, A. S. Davis, and R. Galvez. 2013. 'Elevated Arc/Arg 3.1 protein expression in the basolateral amygdala following auditory trace-cued fear conditioning', *Neurobiol Learn Mem*, 106: 127-33.

Chau, L. S., A. V. Prakapenka, L. Zendeli, A. S. Davis, and R. Galvez. 2014. 'Training-dependent associative learning induced neocortical structural plasticity: a trace eyeblink conditioning analysis', *PLoS One*, 9: e95317.

Cheng, C., M. Sourial, and L. C. Doering. 2012. 'Astrocytes and developmental plasticity in fragile X', *Neural Plast*, 2012: 197491.

Collin, C., K. Miyaguchi, and M. Segal. 1997. 'Dendritic spine density and LTP induction in cultured hippocampal slices', *J Neurophysiol*, 77: 1614-23.

Collins, S. M., A. P. Belagodu, S. L. Reed, and R. Galvez. 2017. 'SHANK1 is differentially expressed during development in CA1 hippocampal neurons and astrocytes', *Dev Neurobiol*.

Comery, Thomas A., Jennifer B. Harris, Patrick J. Willems, Ben A. Oostra, Scott A. Irwin, Ivan Jeanne Weiler, and William T. Greenough. 1997. 'Abnormal dendritic spines in fragile X knockout mice: Maturation and pruning deficits', *Proc Natl Acad Sci U S A*, 94: 5401-04.

Dailey, M. E., and S. J. Smith. 1996. 'The dynamics of dendritic structure in developing hippocampal slices', *J Neurosci*, 16: 2983-94.

Dalzell, L., S. Connor, M. Penner, M. J. Saari, J. C. Leboutillier, and A. C. Weeks. 2011. 'Fear conditioning is associated with synaptogenesis in the lateral amygdala', *Synapse*, 65: 513-9.

De Pitta, M., V. Volman, H. Berry, and E. Ben-Jacob. 2011. 'A tale of two stories: astrocyte regulation of synaptic depression and facilitation', *PLoS Comput Biol*, 7: e1002293.

De Roo, M., P. Klauser, P. M. Garcia, L. Poglia, and D. Muller. 2008. 'Spine dynamics and synapse remodeling during LTP and memory processes', *Prog Brain Res*, 169: 199-207.

Durand, C. M., J. Perroy, F. Loll, D. Perrais, L. Fagni, T. Bourgeron, M. Montcouquiol, and N. Sans. 2012. 'SHANK3 mutations identified in autism lead to modification of dendritic spine morphology via an actin-dependent mechanism', *Mol Psychiatry*, 17: 71-84.

Edmonson, Catherine, Mark N. Ziats, and Owen M. Rennert. 2014. 'Altered glial marker expression in autistic post-mortem prefrontal cortex and cerebellum', *Molecular Autism*, 5: 3-3.

Elibol-Can, B., E. Kilic, S. Yuruker, and E. Jakubowska-Dogru. 2014. 'Investigation into the effects of prenatal alcohol exposure on postnatal spine development and expression of synaptophysin and PSD95 in rat hippocampus', *Int J Dev Neurosci*, 33: 106-14.

Faber, K. M., and J. H. Haring. 1999. 'Synaptogenesis in the postnatal rat fascia dentata is influenced by 5-HT1a receptor activation', *Brain Res Dev Brain Res*, 114: 245-52.

Federmeier, K. D., J. A. Kleim, and W. T. Greenough. 2002. 'Learning-induced multiple synapse formation in rat cerebellar cortex', *Neurosci Lett*, 332: 180-4.

Fiala, J. C., M. Feinberg, V. Popov, and K. M. Harris. 1998. 'Synaptogenesis via dendritic filopodia in developing hippocampal area CA1', *J Neurosci*, 18: 8900-11.

Fortin, D. A., M. A. Davare, T. Srivastava, J. D. Brady, S. Nygaard, V. A. Derkach, and T. R. Soderling. 2010. 'Long-term potentiation-dependent spine enlargement requires synaptic Ca2+-permeable AMPA receptors recruited by CaM-kinase I', *J Neurosci*, 30: 11565-75.

Galvez, R., A. R. Gopal, and W. T. Greenough. 2003. 'Somatosensory cortical barrel dendritic abnormalities in a mouse model of the fragile X mental retardation syndrome', *Brain Res*, 971: 83-9.

Galvez, R., and W. T. Greenough. 2005. 'Sequence of abnormal dendritic spine development in primary somatosensory cortex of a mouse model of the fragile X mental retardation syndrome', *Am J Med Genet A*, 135: 155-60.

Galvez, R., A. P. Weible, and J. F. Disterhoft. 2007. 'Cortical barrel lesions impair whisker-CS trace eyeblink conditioning', *Learn Mem*, 14: 94-100.

Galvez, R., C. Weiss, S. Cua, and J. Disterhoft. 2009. 'A novel method for precisely timed stimulation of mouse whiskers in a freely moving preparation: application for delivery of the conditioned stimulus in trace eyeblink conditioning', *J Neurosci Methods*, 177: 434-9.

Geinisman, Y., R. W. Berry, J. F. Disterhoft, J. M. Power, and E. A. Van der Zee. 2001. 'Associative learning elicits the formation of multiple-synapse boutons', *J Neurosci*, 21: 5568-73.

Gottlieb, J. P., and A. Keller. 1997. 'Intrinsic circuitry and physiological properties of pyramidal neurons in rat barrel cortex', *Exp Brain Res*, 115: 47-60.

Grabrucker, A. M., M. J. Knight, C. Proepper, J. Bockmann, M. Joubert, M. Rowan, G. U. Nienhaus, C. C. Garner, J. U. Bowie, M. R. Kreutz, E. D. Gundelfinger, and T. M. Boeckers. 2011. 'Concerted action of zinc and ProSAP/Shank in synaptogenesis and synapse maturation', *Embo j*, 30: 569-81.

Greenough, W. T., J. M. Juraska, and F. R. Volkmar. 1979. 'Maze training effects on dendritic branching in occipital cortex of adult rats', *Behav Neural Biol*, 26: 287-97.

Greenough, W. T., F. R. Volkmar, and J. M. Juraska. 1973. 'Effects of rearing complexity on dendritic branching in frontolateral and temporal cortex of the rat', *Exp Neurol*, 41: 371-8.

Grossman, A. W., G. M. Aldridge, K. J. Lee, M. K. Zeman, C. S. Jun, H. S. Azam, T. Arii, K. Imoto, W. T. Greenough, and I. J. Rhyu. 2010. 'Developmental characteristics of dendritic spines in the dentate gyrus of Fmr1 knockout mice', *Brain Res*, 1355: 221-7.

Halbedl, S., M. Schoen, M. S. Feiler, T. M. Boeckers, and M. J. Schmeisser. 2016. 'Shank3 is localized in axons and presynaptic specializations of developing hippocampal neurons and involved in the modulation of NMDA receptor levels at axon terminals', *J Neurochem*, 137: 26-32.

Hardingham, N. R., T. Gould, and K. Fox. 2011. 'Anatomical and sensory experiential determinants of synaptic plasticity in layer 2/3 pyramidal neurons of mouse barrel cortex', *J Comp Neurol*, 519: 2090-124.

Harris, K. M., F. E. Jensen, and B. Tsao. 1992. 'Three-dimensional structure of dendritic spines and synapses in rat hippocampus (CA1) at postnatal day 15 and adult ages: implications for the maturation of synaptic physiology and long-term potentiation', *J Neurosci*, 12: 2685-705.

Heinrichs, S. C., K. A. Leite-Morris, M. D. Guy, L. R. Goldberg, A. J. Young, and G. B. Kaplan. 2013. 'Dendritic structural plasticity in the basolateral amygdala after fear conditioning and its extinction in mice', *Behav Brain Res*, 248: 80-4.

Heise, C., J. C. Schroeder, M. Schoen, S. Halbedl, D. Reim, S. Woelfle, M. R. Kreutz, M. J. Schmeisser, and T. M. Boeckers. 2016. 'Selective Localization of Shanks to VGLUT1-Positive Excitatory Synapses in the Mouse Hippocampus', *Front Cell Neurosci*, 10: 106.

Higashimori, H., C. S. Schin, M. S. Chiang, L. Morel, T. A. Shoneye, D. L. Nelson, and Y. Yang. 2016. 'Selective Deletion of Astroglial FMRP Dysregulates Glutamate Transporter

GLT1 and Contributes to Fragile X Syndrome Phenotypes In Vivo', *J Neurosci*, 36: 7079-94.

Holtmaat, A. J., J. T. Trachtenberg, L. Wilbrecht, G. M. Shepherd, X. Zhang, G. W. Knott, and K. Svoboda. 2005. 'Transient and persistent dendritic spines in the neocortex in vivo', *Neuron*, 45: 279-91.

Holtmaat, A., L. Wilbrecht, G. W. Knott, E. Welker, and K. Svoboda. 2006. 'Experience-dependent and cell-type-specific spine growth in the neocortex', *Nature*, 441: 979-83.

Hung, A. Y., K. Futai, C. Sala, J. G. Valtschanoff, J. Ryu, M. A. Woodworth, F. L. Kidd, C. C. Sung, T. Miyakawa, M. F. Bear, R. J. Weinberg, and M. Sheng. 2008. 'Smaller dendritic spines, weaker synaptic transmission, but enhanced spatial learning in mice lacking Shank1', *J Neurosci*, 28: 1697-708.

Irwin, S. A., B. Patel, M. Idupulapati, J. B. Harris, R. A. Crisostomo, B. P. Larsen, F. Kooy, P. J. Willems, P. Cras, P. B. Kozlowski, R. A. Swain, I. J. Weiler, and W. T. Greenough. 2001. 'Abnormal dendritic spine characteristics in the temporal and visual cortices of patients with fragile-X syndrome: a quantitative examination', *Am J Med Genet*, 98: 161-7.

Juraska, J. M. 1982. 'The development of pyramidal neurons after eye opening in the visual cortex of hooded rats: a quantitative study', *J Comp Neurol*, 212: 208-13.

Kharazia, V. N., K. D. Phend, A. Rustioni, and R. J. Weinberg. 1996. 'EM colocalization of AMPA and NMDA receptor subunits at synapses in rat cerebral cortex', *Neurosci Lett*, 210: 37-40.

Killackey, H., and F. Ebner. 1973. 'Convergent projection of three separate thalamic nuclei on to a single cortical area', *Science*, 179: 283-5.

Killackey, H. P., and G. R. Belford. 1979. 'The formation of afferent patterns in the somatosensory cortex of the neonatal rat', *J Comp Neurol*, 183: 285-303.

Kim, J. J., R. E. Clark, and R. F. Thompson. 1995. 'Hippocampectomy impairs the memory of recently, but not remotely, acquired trace eyeblink conditioned responses', *Behav Neurosci*, 109: 195-203.

Kirov, S. A., C. A. Goddard, and K. M. Harris. 2004. 'Age-dependence in the homeostatic upregulation of hippocampal dendritic spine number during blocked synaptic transmission', *Neuropharmacology*, 47: 640-8.

Kleim, J. A., E. Lussnig, E. R. Schwarz, T. A. Comery, and W. T. Greenough. 1996. 'Synaptogenesis and Fos expression in the motor cortex of the adult rat after motor skill learning', *J Neurosci*, 16: 4529-35.

Knott, G. W., C. Quairiaux, C. Genoud, and E. Welker. 2002. 'Formation of dendritic spines with GABAergic synapses induced by whisker stimulation in adult mice', *Neuron*, 34: 265-73.

Kuhlman, S. J., D. H. O'Connor, K. Fox, and K. Svoboda. 2014a. 'Structural plasticity within the barrel cortex during initial phases of whisker-dependent learning', *J Neurosci*, 34: 6078-83.

Kuhlman, Sandra J., Daniel H. O'Connor, Kevin Fox, and Karel Svoboda. 2014b. 'Structural Plasticity within the Barrel Cortex during Initial Phases of Whisker-Dependent Learning', *The Journal of Neuroscience*, 34: 6078-83.

Lennertz, L., M. Wagner, W. Wolwer, A. Schuhmacher, I. Frommann, J. Berning, S. Schulze-Rauschenbach, M. W. Landsberg, A. Steinbrecher, M. Alexander, P. E. Franke, R. Pukrop, S. Ruhrmann, A. Bechdolf, W. Gaebel, J. Klosterkotter, H. Hafner, W. Maier, and R. Mossner. 2012. 'A promoter variant of SHANK1 affects auditory working

memory in schizophrenia patients and in subjects clinically at risk for psychosis', *Eur Arch Psychiatry Clin Neurosci*, 262: 117-24.

Leuner, B., J. Falduto, and T. J. Shors. 2003. 'Associative memory formation increases the observation of dendritic spines in the hippocampus', *J Neurosci*, 23: 659-65.

Li, M., Z. Cui, Y. Niu, B. Liu, W. Fan, D. Yu, and J. Deng. 2010. 'Synaptogenesis in the developing mouse visual cortex', *Brain Res Bull*, 81: 107-13.

Lim, S., S. Naisbitt, J. Yoon, J. I. Hwang, P. G. Suh, M. Sheng, and E. Kim. 1999. 'Characterization of the Shank family of synaptic proteins. Multiple genes, alternative splicing, and differential expression in brain and development', *J Biol Chem*, 274: 29510-8.

Loh, R., L. Chau, A. Aijaz, K. Wu, and R. Galvez. 2017. 'Antagonizing the different stages of kappa opioid receptor activation selectively and independently attenuates acquisition and consolidation of associative memories', *Behav Brain Res*, 323: 1-10.

Lomo, T. 1971. 'Patterns of activation in a monosynaptic cortical pathway: the perforant path input to the dentate area of the hippocampal formation', *Exp Brain Res*, 12: 18-45.

Lubke, J., V. Egger, B. Sakmann, and D. Feldmeyer. 2000. 'Columnar organization of dendrites and axons of single and synaptically coupled excitatory spiny neurons in layer 4 of the rat barrel cortex', *J Neurosci*, 20: 5300-11.

Ma, L., Q. Qiao, J. W. Tsai, G. Yang, W. Li, and W. B. Gan. 2016. 'Experience-dependent plasticity of dendritic spines of layer 2/3 pyramidal neurons in the mouse cortex', *Dev Neurobiol*, 76: 277-86.

Markus, E. J., T. L. Petit, and J. C. LeBoutillier. 1987. 'Synaptic structural changes during development and aging', *Brain Res*, 432: 239-48.

Martel, G., R. Jaffard, and J. L. Guillou. 2010. 'Identification of hippocampus-dependent and hippocampus independent memory components in step-down inhibitory avoidance tasks', *Behav Brain Res*, 207: 138-43.

Mashayekhi, F., N. Mizban, E. Bidabadi, and Z. Salehi. 2016. 'The association of SHANK3 gene polymorphism and autism', *Minerva Pediatr*.

Matt, S. M., M. A. Lawson, and R. W. Johnson. 2016. 'Aging and peripheral lipopolysaccharide can modulate epigenetic regulators and decrease IL-1beta promoter DNA methylation in microglia', *Neurobiol Aging*, 47: 1-9.

Melo, L. L., M. L. Brandao, F. G. Graeff, and G. Sandner. 1997. 'Bilateral ablation of the auditory cortex in the rat alters conditioned emotional suppression to a sound as appraised through a latent inhibition study', *Behav Brain Res*, 88: 59-65.

Naisbitt, S., E. Kim, J. C. Tu, B. Xiao, C. Sala, J. Valtschanoff, R. J. Weinberg, P. F. Worley, and M. Sheng. 1999. 'Shank, a novel family of postsynaptic density proteins that binds to the NMDA receptor/PSD-95/GKAP complex and cortactin', *Neuron*, 23: 569-82.

O'Malley, A., C. O'Connell, K. J. Murphy, and C. M. Regan. 2000. 'Transient spine density increases in the mid-molecular layer of hippocampal dentate gyrus accompany consolidation of a spatial learning task in the rodent', *Neuroscience*, 99: 229-32.

O'Malley, A., C. O'Connell, and C. M. Regan. 1998. 'Ultrastructural analysis reveals avoidance conditioning to induce a transient increase in hippocampal dentate spine density in the 6 hour post-training period of consolidation', *Neuroscience*, 87: 607-13.

Orner, D. A., C. C. Chen, D. E. Orner, and J. C. Brumberg. 2014. 'Alterations of dendritic protrusions over the first postnatal year of a mouse: an analysis in layer VI of the barrel cortex', *Brain Struct Funct*, 219: 1709-20.

Pacey, L. K., S. Guan, S. Tharmalingam, C. Thomsen, and D. R. Hampson. 2015. 'Persistent astrocyte activation in the fragile X mouse cerebellum', *Brain Behav*, 5: e00400.

Peca, J., C. Feliciano, J. T. Ting, W. Wang, M. F. Wells, T. N. Venkatraman, C. D. Lascola, Z. Fu, and G. Feng. 2011. 'Shank3 mutant mice display autistic-like behaviours and striatal dysfunction', *Nature*, 472: 437-42.

Petersen, C. C. 2003. 'The barrel cortex--integrating molecular, cellular and systems physiology', *Pflugers Arch*, 447: 126-34.

Pick, J. E., M. Malumbres, and E. Klann. 2012. 'The E3 ligase APC/C-Cdh1 is required for associative fear memory and long-term potentiation in the amygdala of adult mice', *Learn Mem*, 20: 11-20.

Pocock, J. M., and H. Kettenmann. 2007. 'Neurotransmitter receptors on microglia', *Trends Neurosci*, 30: 527-35.

Reemst, K., S. C. Noctor, P. J. Lucassen, and E. M. Hol. 2016. 'The Indispensable Roles of Microglia and Astrocytes during Brain Development', *Front Hum Neurosci*, 10: 566.

Restivo, L., G. Vetere, B. Bontempi, and M. Ammassari-Teule. 2009. 'The formation of recent and remote memory is associated with time-dependent formation of dendritic spines in the hippocampus and anterior cingulate cortex', *J Neurosci*, 29: 8206-14.

Sala, C., V. Piech, N. R. Wilson, M. Passafaro, G. Liu, and M. Sheng. 2001. 'Regulation of dendritic spine morphology and synaptic function by Shank and Homer', *Neuron*, 31: 115-30.

Sato, D., A. C. Lionel, C. S. Leblond, A. Prasad, D. Pinto, S. Walker, I. O'Connor, C. Russell, I. E. Drmic, F. F. Hamdan, J. L. Michaud, V. Endris, R. Roeth, R. Delorme, G. Huguet, M. Leboyer, M. Rastam, C. Gillberg, M. Lathrop, D. J. Stavropoulos, E. Anagnostou, R.

Weksberg, E. Fombonne, L. Zwaigenbaum, B. A. Fernandez, W. Roberts, G. A. Rappold, C. R. Marshall, T. Bourgeron, P. Szatmari, and S. W. Scherer. 2012. 'SHANK1 Deletions in Males with Autism Spectrum Disorder', *Am J Hum Genet*, 90: 879-87.

Schachtele, S. J., J. Losh, M. E. Dailey, and S. H. Green. 2011. 'Spine formation and maturation in the developing rat auditory cortex', *J Comp Neurol*, 519: 3327-45.

Schenk, F., and R. G. Morris. 1985. 'Dissociation between components of spatial memory in rats after recovery from the effects of retrohippocampal lesions', *Exp Brain Res*, 58: 11-28.

Schutt, J., K. Falley, D. Richter, H. J. Kreienkamp, and S. Kindler. 2009. 'Fragile X mental retardation protein regulates the levels of scaffold proteins and glutamate receptors in postsynaptic densities', *J Biol Chem*, 284: 25479-87.

Scully, D., R. Fedriani, I. E. Desouza, K. J. Murphy, and C. M. Regan. 2012. 'Regional dissociation of paradigm-specific synapse remodeling during memory consolidation in the adult rat dentate gyrus', *Neuroscience*, 209: 74-83.

Seifert, G., M. Zhou, and C. Steinhauser. 1997. 'Analysis of AMPA receptor properties during postnatal development of mouse hippocampal astrocytes', *J Neurophysiol*, 78: 2916-23.

Sheng, M., and E. Kim. 2000. 'The Shank family of scaffold proteins', *J Cell Sci*, 113 (Pt 11): 1851-6.

Singer, B. F., N. Bubula, D. Li, M. M. Przybycien-Szymanska, V. P. Bindokas, and P. Vezina. 2016. 'Drug-Paired Contextual Stimuli Increase Dendritic Spine Dynamics in Select Nucleus Accumbens Neurons', *Neuropsychopharmacology*, 41: 2178-87.

Sirevaag, A. M., and W. T. Greenough. 1985. 'Differential rearing effects on rat visual cortex synapses. II. Synaptic morphometry', *Brain Res*, 351: 215-26.

Sloviter, R. S., and T. Lomo. 2012. 'Updating the lamellar hypothesis of hippocampal organization', *Front Neural Circuits*, 6: 102.

Spacek, J., and K. M. Harris. 1997. 'Three-dimensional organization of smooth endoplasmic reticulum in hippocampal CA1 dendrites and dendritic spines of the immature and mature rat', *J Neurosci*, 17: 190-203.

Stella, N., M. Tence, J. Glowinski, and J. Premont. 1994. 'Glutamate-evoked release of arachidonic acid from mouse brain astrocytes', *J Neurosci*, 14: 568-75.

Sungur, A. O., R. K. Schwarting, and M. Wohr. 2016. 'Early communication deficits in the Shank1 knockout mouse model for autism spectrum disorder: Developmental aspects and effects of social context', *Autism Res*, 9: 696-709.

Takehara, K., S. Kawahara, K. Takatsuki, and Y. Kirino. 2002. 'Time-limited role of the hippocampus in the memory for trace eyeblink conditioning in mice', *Brain Res*, 951: 183-90.

Tassone, F., K. P. Iong, T. H. Tong, J. Lo, L. W. Gane, E. Berry-Kravis, D. Nguyen, L. Y. Mu, J. Laffin, D. B. Bailey, and R. J. Hagerman. 2012. 'FMR1 CGG allele size and prevalence ascertained through newborn screening in the United States', *Genome Med*, 4: 100.

Tay, T. L., J. C. Savage, C. W. Hui, K. Bisht, and M. E. Tremblay. 2017. 'Microglia across the lifespan: from origin to function in brain development, plasticity and cognition', *J Physiol*, 595: 1929-45.

Tseng, W., R. Guan, J. F. Disterhoft, and C. Weiss. 2004. 'Trace eyeblink conditioning is hippocampally dependent in mice', *Hippocampus*, 14: 58-65.

Tu, J. C., B. Xiao, S. Naisbitt, J. P. Yuan, R. S. Petralia, P. Brakeman, A. Doan, V. K. Aakalu, A. A. Lanahan, M. Sheng, and P. F. Worley. 1999. 'Coupling of mGluR/Homer and PSD-95 complexes by the Shank family of postsynaptic density proteins', *Neuron*, 23: 583-92.

Turner, A. M., and W. T. Greenough. 1985. 'Differential rearing effects on rat visual cortex synapses. I. Synaptic and neuronal density and synapses per neuron', *Brain Res*, 329: 195-203.

Verkhratsky, A., and F. Kirchhoff. 2007. 'NMDA Receptors in glia', *Neuroscientist*, 13: 28-37.

Wang, X., P. A. McCoy, R. M. Rodriguiz, Y. Pan, H. S. Je, A. C. Roberts, C. J. Kim, J. Berrios, J. S. Colvin, D. Bousquet-Moore, I. Lorenzo, G. Wu, R. J. Weinberg, M. D. Ehlers, B. D. Philpot, A. L. Beaudet, W. C. Wetsel, and Y. H. Jiang. 2011. 'Synaptic dysfunction and abnormal behaviors in mice lacking major isoforms of Shank3', *Hum Mol Genet*, 20: 3093-108.

White, S. R. 1974. 'Atropine, scopolamine and hippocampal lesion effects on alternation performance of rats', *Pharmacol Biochem Behav*, 2: 297-307.

Wilbrecht, L., A. Holtmaat, N. Wright, K. Fox, and K. Svoboda. 2010. 'Structural plasticity underlies experience-dependent functional plasticity of cortical circuits', *J Neurosci*, 30: 4927-32.

Withers, G. S., J. R. Farley, J. R. Sterritt, A. B. Crane, and C. S. Wallace. 2017. 'Interactions with Astroglia Influence the Shape of the Developing Dendritic Arbor and Restrict Dendrite Growth Independent of Promoting Synaptic Contacts', *PLoS One*, 12: e0169792.

Withers, G. S., and W. T. Greenough. 1989. 'Reach training selectively alters dendritic branching in subpopulations of layer II-III pyramids in rat motor-somatosensory forelimb cortex', *Neuropsychologia*, 27: 61-9.

Woolsey, T. A., and H. Van der Loos. 1970. 'The structural organization of layer IV in the somatosensory region (SI) of mouse cerebral cortex. The description of a cortical field composed of discrete cytoarchitectonic units', *Brain Res*, 17: 205-42.

Zhang, Y., C. M. Gaetano, K. R. Williams, G. J. Bassell, and M. R. Mihailescu. 2014. 'FMRP interacts with G-quadruplex structures in the 3'-UTR of its dendritic target Shank1 mRNA', *RNA Biol*, 11: 1364-74.